LEUPHANA
UNIVERSITÄT LÜNEBURG

Bachelor Thesis Major Environmental Sciences (B. Sc.)

Ready and Inherent Biodegradability of Sparfloxacin and its Phototransformation Products

---

First Reviewer: Morten Suk, M. Sc.
Second Reviewer: Dr. Ing. Oliver Olsson
Faculty of Sustainability
Institute of Sustainable and Environmental Chemistry (ISEC)

Submitted by:
Merle Käberich
Matriculation Number: 3029727
Werneckestr. 35, 37603 Holzminden
merle.kaeberich@stud.leuphana.de

Date of Submission: 13th of August 2019

Abstract

Fluoroquinolone antibiotics are frequently used in both human and veterinary medicine. The second generation fluoroquinolone sparfloxacin is mostly applied to treat respiratory tract infections. Like many pharmaceuticals, the drug is not completely metabolised after uptake. Due to the non-biodegradability of sparfloxacin, it can be detected in the aquatic environment, leading to toxic effects on non-target organisms as well as the development of resistant bacteria. To target the problem of persistent pharmaceuticals in the environment, the "Benign by Design" approach aims at the development of compounds with improved biodegradability and retained pharmacological properties.

In this thesis, it was determined if sparfloxacin and its phototransformation products resulting from UV irradiation differ in their ready and inherent biodegradability. For this purpose, the Closed Bottle Test (OECD 301 D) and the Zahn-Wellens Test (OECD 302 B) were performed in combination with HPLC analysis. In the Closed Bottle Test, neither sparfloxacin nor any of the phototransformation products were readily biodegradable. During the Zahn-Wellens Test, the test substances were subject to major adsorption to the sewage sludge. Sparfloxacin was degraded in several test bottles within the last week of the test and multiple new substances emerged through processes of biotransformation. Several detected transformation products displayed potentially improved degradability through abiotic degradation processes and biodegradation. Especially the transformation products demonstrating biodegradation in all test bottles are of interest, because these findings contribute to the "Benign by Design" concept and the knowledge on biodegradability. Further research concerning the identification of the promising derivatives as well as a determination of their pharmacological and toxicological properties is recommendable.

Table of Contents

List of Figures i
List of Tables ii
List of Abbreviations iii
1. Introduction 1
2. Theoretical Background and State of Research 3
2.1. Fluoroquinolones 3
2.1.1. Sparfloxacin 5
2.2. "Benign by Design": Non-Targeted Derivatisation by Photodegradation 6
2.3. Biodegradation 8
2.3.1. Closed Bottle Test 9
2.3.2. Zahn-Wellens Test 10
3. Materials and Methodology 10
3.1. Required Instruments and Reagents 10
3.2. Photodegradation of Sparfloxacin 12
3.3. DOC and HPLC Measurement 12
3.4. Closed Bottle Test 13
3.5. Zahn-Wellens Test 15
4. Results and Discussion 17
4.1. Photodegradation of Sparfloxacin 17
4.2. Closed Bottle Test 21
4.2.1. Biodegradation Closed Bottle Test Determined by O_2 Consumption 21
4.2.2. Biodegradation Closed Bottle Test Determined by HPLC Analysis 23
4.3. Zahn-Wellens Test 25
4.3.1. Degradation Zahn-Wellens Test Determined by DOC Measurements 25
4.3.2. Abiotic Degradation Zahn-Wellens Test Determined by HPLC Analysis 29
4.3.3. Biodegradation Zahn-Wellens Test Determined by HPLC Analysis 31
4.3.3.1. Development of SPX 32
4.3.3.2. Development of Transformation Products in SPX_0 33
4.3.3.3. Development of Relevant Transformation Products in SPX_{128} and SPX_{256} 34
4.4. Implications for "Benign by Design" 38
5. Conclusion 39
6. Literature 41
7. Annex I
8. Declaration of Authorship XI

List of Figures

Fig. 1: Schematic depiction of the approach conducted in this thesis 2
Fig. 2: First quinolone antibiotic (nalidixic acid), FQs from different generations and general structure of FQs 3
Fig. 3: Molecular structure (left) and crystal structure (right) of FQ binding to topoisomerase IV of *A. baumannii* (from Aldred et al., 2014). 4
Fig. 4: Structure of SPX 6
Fig. 5: Examples of photo-TPs of SPX (from Engler et al., 1998; Hubicka et al., 2013) 7
Fig. 6: Calibration curve absorbance and COD, applicable for COD cell test Spectroquant®, 5–80 mg L^{-1}, model CSB01796, lot number HC873121 13
Fig. 7: Setup ZWT 17
Fig. 8: SPX solution after 128 min (left) and 256 min (right) of photolysis 17
Fig. 9: SPX and DOC development during 256 min (red) and 496 min (blue) irradiation with UV light 18
Fig. 10: Absorbance spectrum of SPX, measured with PDA detector, 230–600 nm 19
Fig. 11: Emittance spectrum of the applied medium pressure UV lamp, type TQ 150, from Heraeus, Germany 19
Fig. 12: Development of photo-TPs SPX during 256 min irradiation with UV light 20
Fig. 13: Development of photo-TPs SPX during 496 min irradiation with UV light 20
Fig. 14: Biodegradation of test substances, toxicity controls and QC during CBT over test duration of 28 days 22
Fig. 15: SPX development during CBT; SPX peak areas of 0 (blue) and 28 (red) days measurements are depicted 24
Fig. 16: Development of photo-TPs 1–22 in SPX_{128} during CBT; TP peak areas of 0 (blue) and 28 (red) days measurements are depicted 24
Fig. 17: Development of photo-TPs 1–22 in SPX_{256} during CBT; TP peak areas of 0 (blue) and 28 (red) days measurements are depicted 25
Fig. 18: Degradation of test substances, toxicity controls, sterile controls and QC during ZWT over test duration of 28 days; 3 h measurements taken as start value 26
Fig. 19: Degradation of test substances and toxicity controls during ZWT over test duration of 28 days; theoretical DOC taken as start value 26
Fig. 20: SPX development in sterile controls during ZWT over test duration of 28 days 29
Fig. 21: Development of TPs decreasing in SPX_{128} St and SPX_{256} St during ZWT over test duration of 28 days 30
Fig. 22: Possible hydrolytically unstable and strong reducing TPs of SPX 31
Fig. 23: SPX development in SPX_0, SPX_{128} and SPX_{256} during ZWT over test duration of 28 days 32
Fig. 24: Development of TPs in SPX_0 with peak area $< 5 \cdot 10^5$ during ZWT over test duration of 28 days 34
Fig. 25: Development of TPs in SPX_0 with peak area $> 5 \cdot 10^5$ during ZWT over test duration of 28 days 34
Fig. 26: Development of newly emerging TPs in SPX_{128} and SPX_{256} during ZWT over test duration of 28 days 35

Fig. 27: Development of increasing TPs in SPX_{128} and SPX_{256} with peak area < $2 \cdot 10^6$ during ZWT over test duration of 28 days 36
Fig. 28: Development of increasing TPs in SPX_{128} and SPX_{256} with peak area > $2 \cdot 10^6$ during ZWT over test duration of 28 days 36
Fig. 29: Development of decreasing TPs in SPX_{128} and SPX_{256} with peak area < $2 \cdot 10^6$ during ZWT over test duration of 28 days 37
Fig. 30: Development of decreasing TPs in SPX_{128} and SPX_{256} with peak area > $2 \cdot 10^6$ during ZWT over test duration of 28 days 38

List of Tables

Tab. 1: MIC values of SPX (from Pankuch et al., 1996) 6
Tab. 2: Biodegradability of various FQs 9
Tab. 3: Required instruments 10
Tab. 4: Required reagents 11
Tab. 5: Substances added in the CBT 14
Tab. 6: Substances added in the ZWT 16

List of Abbreviations

API	active pharmaceutical ingredient
BOD	biological oxygen demand
BV	blank value
CBT	Closed Bottle Test
COD	chemical oxygen demand
DAD	diode array detector
DEG	diethylene glycol
DOC	dissolved organic carbon
FQ	fluoroquinolone
HPLC	high performance liquid chromatography
K_{ow}	octanol-water partition coefficient
MIC	minimum inhibitory concentration
OECD	Organisation for Economic Cooperation and Development
PDA	photo diode array
PES	polyether sulfone
PFP	pentafluorophenyl
QC	quality control
QSAR	quantitative structure-activity relationships
sol.	solution
SPX	sparfloxacin
SPX_0	unirradiated sparfloxacin solution
SPX_{128}	sparfloxacin solution irradiated with UV light for 128 min
SPX_{256}	sparfloxacin solution irradiated with UV light for 256 min
St	sterile control
ThOD	theoretical oxygen demand
TOC	total organic carbon
Tox	toxicity control
TP	transformation product
UV	ultra-violet
VIS	visible light
WWTP	wastewater treatment plant
ZWT	Zahn-Wellens Test

1. Introduction

The use of antibiotics and pharmaceuticals in general has been subject to a continuous increase in the recent decades in both human and veterinary medicine (e.g. Bergmann et al., 2011). With the ongoing demographic change and increasing life expectancy, as well as a growing world population, this trend can be expected to continue in the future. Most pharmaceuticals are not completely metabolised after uptake by humans or animals and therefore, a part of the active pharmaceutical ingredient (API) is excreted more or less unmodified. Even though the APIs emitted by humans undergo various steps in wastewater treatment plants (WWTPs), they can often not be removed substantially due to their persistence. This leads to their occurrence in surface water, where the concentrations measured in Germany range between less than 0.1 µg L^{-1} and more than 1.0 µg L^{-1} (Klatte et al., 2017). Once present in the surface water, the APIs can unfold their potentially damaging effects on the environment and water organisms. Approximately half of the 2300 approved APIs for human medicine in Germany are considered to be environmentally relevant due to their persistence, potential for bioaccumulation and toxicity (Klatte et al., 2017). Furthermore, the continuous exposure of bacteria to antibiotics fosters the emergence of resistances and therefore endangers the effectiveness of antibiotics, which is relied upon in both human and veterinary medicine. Already, prevalent resistances create the need for the permanent development of new antibiotics to still achieve effects against bacterial strains (Aldred et al., 2014). In addition to this, processes of metabolisation, biodegradation, photolysis, hydrolysis and other abiotic mechanisms can lead to a conversion of the parent compound to transformation products (TPs) which might differ in their characteristics. These arising TPs and the pathways of transformation are difficult to determine and complicate the environmental assessment of the parent compound substantially (Leder et al., 2015). Due to these problems, micro-pollutants (APIs and TPs) are seen as a challenge to sustainable management of water resources. To target these issues, the policy framework Strategic Approach to International Chemicals Management (SAICM) was developed and adopted by the First International Conference on Chemical Management (ICCM1) in 2006. The framework pursues the goal of minimising the adverse effects on humans and the environment arising from the production and use of chemicals by 2020. To achieve this minimisation, a sound management of the chemicals throughout their life cycle is necessary (aus der Beek et al., 2016). With policies targeting the previously described problems, the relevance of pharmaceuticals in the environment for sustainable development is increasingly brought to attention. However, the research area of sustainable chemistry and pharmacy is still a

relatively new field and sustainability considerations are just starting to be extensively incorporated into the design of pharmaceuticals and chemicals in general.

The antibiotic sparfloxacin (SPX) belongs to the fluoroquinolones (FQs) which are characterised by high potency, a broad spectrum of activity, good bioavailability and potentially low incidence of side effects. Therefore, FQs belong to the worldwide most frequently used antibiotics in both human and veterinary medicine and are prescribed for a wide variety of bacterial infections. For example, ciprofloxacin as one of the most commonly used FQs had a consumption rate of 32979.5 kg in Germany in the year 2009, with an increase of 92% between 2002 and 2009 (Bergmann et al., 2011). SPX is applied to treat respiratory tract infections (Ball, 2000). The frequent use of the antibiotic in animal husbandry has led to detections of SPX concentrations up to 80–180 ng L^{-1} in swine wastewater canals (Yao et al., 2015). SPX and FQs in general have been found to be non-biodegradable (Amorim et al., 2014; Bergheim et al., 2015; Kümmerer et al., 2000a) and photoreactive (e.g. Hubicka et al., 2013), leading to their persistence in the aquatic environment and the formation of TPs.

The goal of this thesis was to determine whether the photo-TPs of SPX display a different potential for biodegradation compared to the initial substance. For this purpose, a non-targeted derivatisation of SPX was conducted by irradiation with UV light. The photolysis solutions as well as the parent compound were then tested for ready biodegradability in the Closed Bottle Test (CBT; OECD 301 D) and for inherent biodegradability in the Zahn-Wellens Test (ZWT; OECD 302 B), with additional sample analysis by HPLC. These experiments followed the “Benign by Design” approach conducted by Rastogi et al. (2014) and pursued the target of determining photo-TPs of SPX displaying improved biodegradability in comparison to the parent compound (see figure 1).

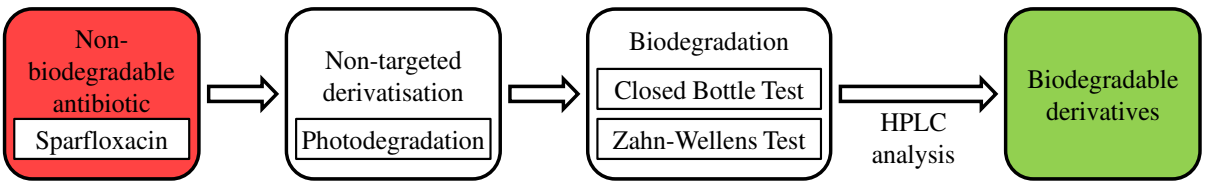

Fig. 1: Schematic depiction of the approach conducted in this thesis

2. Theoretical Background and State of Research

2.1. Fluoroquinolones

In 1962, with the discovery of nalidixic acid, the first quinolone antibiotic came into use. Nalidixic acid was mostly limited to the treatment of gram-negative urinary tract infections. The naphthyridone nucleus of the molecule became the basis for the development of different compounds. From the quinolones, the two substance groups of naphthyridones and FQs were developed (Ball, 2000). In the general structure of FQs (see figure 2), the carboxyl group must be included for binding to the target, while the R_1 substituent controls pharmacokinetics and efficacy. The atom at position X impacts the activity and the R_5 and R_7 substituents control the activity spectrum (Kümmerer, 2007).

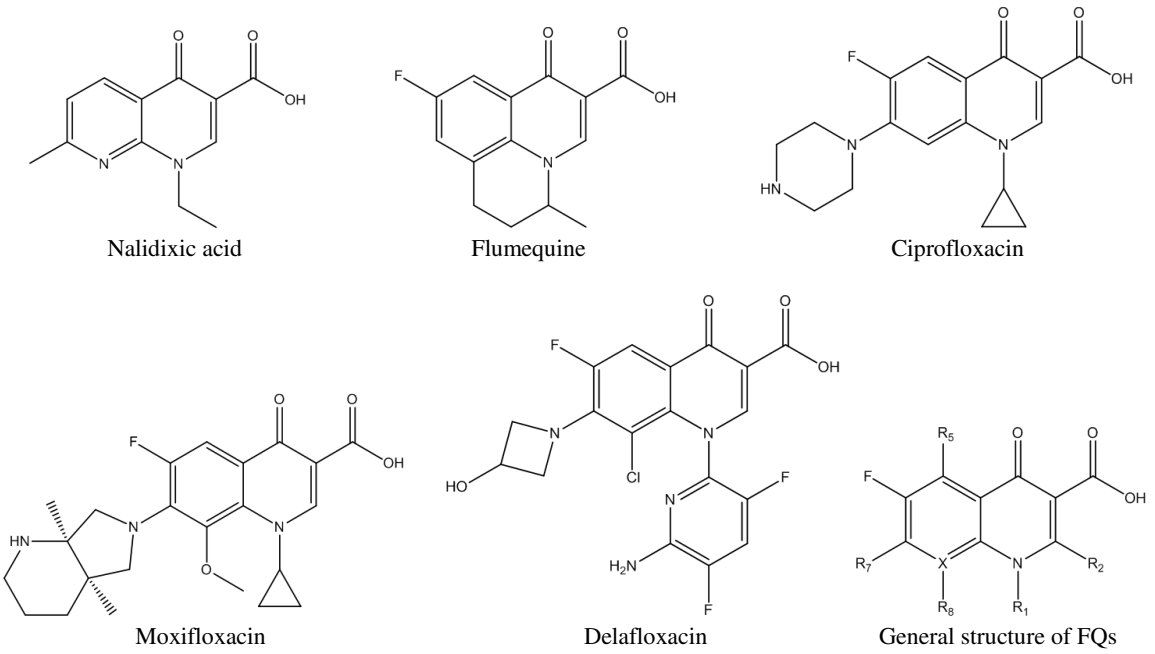

Fig. 2: First quinolone antibiotic (nalidixic acid), FQs from different generations and general structure of FQs

Based on their antibacterial spectrum, FQs can be categorised into different generations (see figure 2). First generation FQs (e.g. flumequine) were predominantly used for the treatment of urinary tract infections. The second generation (e.g. ciprofloxacin, SPX) has enhanced activity against gram-negative pathogens and limited potency against gram-positive pathogens and is used for a wide spectrum of infections. In the third generation (e.g. moxifloxacin) the activity against gram-positive bacteria was enhanced and the fourth generation FQs (e.g. delafloxacin) display increased dual action at the DNA gyrase and topoisomerase IV to decelerate the development of resistances (Ball, 2000; Biswas et al., 2009).

Quinolones effectuate their bactericidal mode of action by targeting the gyrase and topoisomerase IV. These enzymes generate breaks in the bacterial chromosome to control DNA under- and overwinding and to remove knots and tangles (Aldred et al., 2014). The

quinolones inhibit the DNA ligase, leading to the generated breaks not being repaired. This DNA damage causes the SOS response to give the cell time to repair the DNA. When this is not possible, the *mazF* toxin is released by degradation of the corresponding *mazE* antitoxin, leading to oxidative stress and cell destruction. After the point of no return has been reached, this results in cell death (Amitai et al., 2004; Kimmitt et al., 2000). The FQ-enzyme binding is established through a water-metal ion bridge as depicted in figure 3 (Aldred et al., 2014).

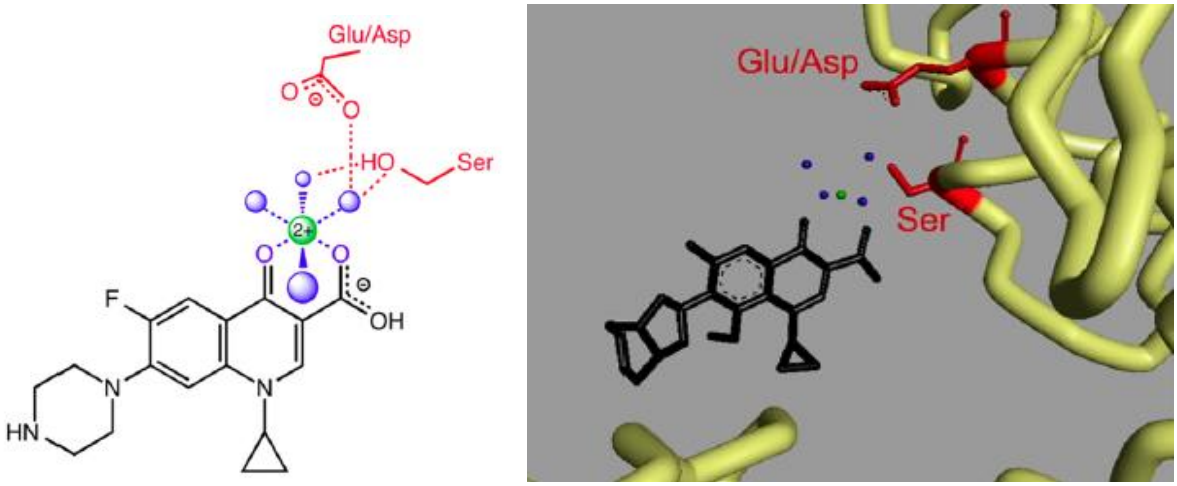

Fig. 3: Molecular structure (left) and crystal structure (right) of FQ binding to topoisomerase IV of *A. baumannii* (from Aldred et al., 2014).
A magnesium cation (green) is coordinated by four water molecules (blue) and two oxygen atoms of the FQ. The water molecules form hydrogen bonds with the serine and acidic side chains of the enzyme (red).

Despite their potency against bacterial infections, FQs have been the target of critical assessments, concentrating on both environmental effects and effects on humans. Side effect reactions are categorised as mild to moderate and can include damage to tendons, joints and the central nervous system (FDA, 2016).

The emission pathway from application in human medicine leads through the human body, where the FQs cannot be completely metabolised, into the wastewater. Due to their persistence, the FQs cannot be degraded in WWTPs and therefore continue to the surface water. Another application is the veterinary use in animal husbandry for the treatment as well as the prevention of diseases (Kümmerer, 2009). The antibiotics can also be applied for growth promotion (Gaskins et al., 2002), which has been banned in the European Union and some other countries. Through the application of manure as a fertiliser in agriculture, as well as through excretions of grazing animals and substance residues in shed dust, the FQs are transported into the environment without the interposition of WWTPs (Hamscher & Hartung, 2008; Kümmerer, 2008).

Typical concentrations of the frequently used ciprofloxacin reach around 7–103 ng L^{-1} in surface water downstream of WWTP discharge (Ferrando-Climent et al., 2014). FQs generally have a high persistence and high sorption potential, leading to the accumulation in

soils, biomass, and sewage sludge (Zhou et al., 2013). Even though, with a median value of log K_{ow} < 2.5, the substances have relatively low octanol-water partition coefficients, their high sorption affinity is established through electrostatic interactions and the amphoteric nature of the molecules, leading to a pH dependency. Accumulation in soils and sewage sludge can lead to decreased soil respiration, thus affecting environmental functions. Additionally, this results in toxicity to non-target organisms as well as increased human uptake through the consumption of contaminated agricultural plants (Taveira Parente et al., 2019; Tervahauta et al., 2014; Thomaidi et al., 2016).

Another consequence of the environmental occurrence is the development of resistant bacteria which are threatening the effectiveness of these antibiotics. These resistances occur through continuous exposure to the FQs and the resulting selection pressure on bacteria populations and are most commonly caused by mutations in the gyrase or topoisomerase IV. The water-metal ion bridge is disrupted, resulting in the observed resistance. In addition to this target-mediated resistance, resistance can also be plasmid- and chromosome-mediated. Due to these mutations, pharmaceutical research is targeting the development of new antibiotics not being dependent on the water-metal ion bridge for primary interaction with the enzymes (Aldred et al., 2014).

2.1.1. Sparfloxacin

SPX belongs to the second generation of FQs. The substance was patented in 1985 and has been in medical use since 1994. As shown in figure 4, a piperazine substituent with two methyl groups is added at position 7. This increases the potency and the antibacterial spectrum, especially being effective against *Pseudomonas aeruginosa*, an important hospital germ which is resistant to multiple antibiotics. At position 1, a cyclopropane substituent is attached. The addition of the amino group at position 5 leads to increased activity against gram-positive bacteria and the fluorine atom at position 8 increases the activity against anaerobic bacteria (Domagala, 1994; Rubinstein, 2001). Besides these structure-activity relationships, the substituents around the quinolone nucleus are also associated with specific side effects. Effects on the central nervous system are considered relatively mild for SPX, due to its low degree of GABA inhibition by the substituent at position 7 and moderate lipophilicity of the substance. However, effects of phototoxicity are observed for SPX, leading to a highest no effect phototoxic dosage of 18 mg kg^{-1} (Domagala, 1994). These effects are mostly caused by the position 8 substituent, with fluorine causing the highest phototoxicity. Additionally, SPX unfolds moderate genetic toxicity with a concentration of

370 mg L^{-1} leading to 50% cytotoxicity, caused by the substituents in positions 5 and 8 (Domagala, 1994).

Tab. 1: MIC values of SPX (from Pankuch et al., 1996)

Bacterial strains	*MIC [µg mL^{-1}]*
Penicillin-susceptible pneumococci	0.25–2.0
Penicillin-intermediate pneumococci	0.125–0.5
Penicillin-resistant pneumococci	0.125–0.5

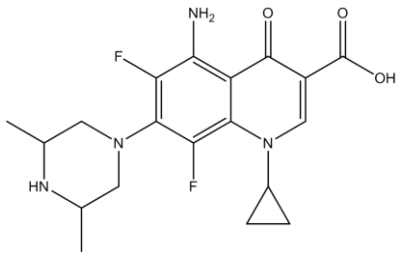

Fig. 4: Structure of SPX

Pankuch et al. (1996) determined the MIC values of SPX for a variety of bacterial strains which are displayed in table 1. In combination with the causation of serious cardiac dysrhythmias, the phototoxic effects of SPX have led to research largely abandoning the development of the drug (Ball, 2000).

2.2. "Benign by Design": Non-Targeted Derivatisation by Photodegradation

Pharmaceuticals and other chemicals in the environment are influenced by processes of photolysis. The substances can either absorb a photon in direct photolysis or react with a sensitizer (e.g. NO_3^-) absorbing the photon in indirect photolysis. The resulting chemical relaxation processes and reactions lead to a degradation of the initial compound (Arnold & McNeill, 2007). If the compound is not completely mineralised, the photodegradation results in the formation of photo-TPs which can differ from the original substance concerning their characteristics, for example their toxicity or biodegradability (Li et al., 2012).

The photoreactivity of a compound is fostered by certain structural functions, including unsaturated bonds, weak bonds between carbon and hydrogen and by carbonyl groups (Fatta-Kassinos et al., 2011). SPX and other FQs have been found to display high photoreactivity. Hubicka et al. (2013) characterised the photodegradation of SPX through UVA irradiation by a first-order reaction, while Engler et al. (1998) stated that SPX reached a constant concentration level after 8 h of irradiation and could not be completely degraded. In several studies, up to nine photo-TPs of SPX have been identified (Engler et al., 1998; Hubicka et al., 2013; Salgado et al., 2009), of which four examples are depicted in figure 5. Photo-TPs of FQs in general have been found to display lower acute ecotoxicity (Bergheim et al., 2015), while not considerably differing in their potential for ready biodegradability (Vasconcelos et al., 2009; Vasquez et al., 2013).

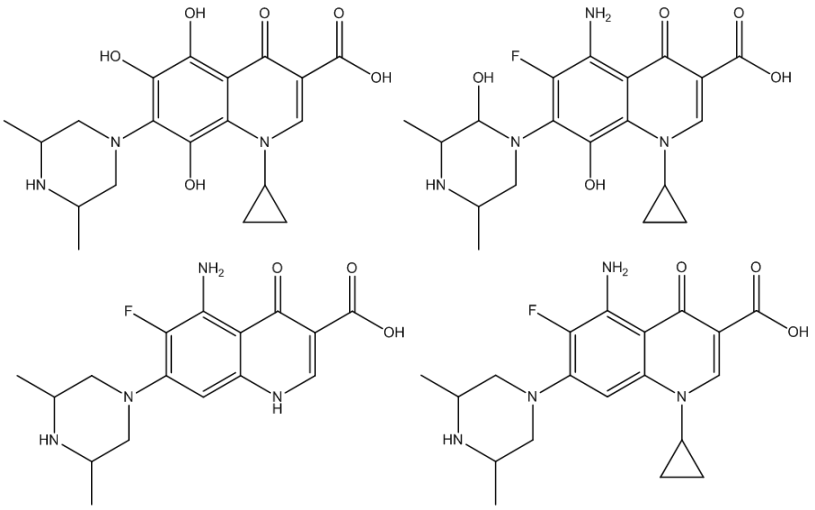

Fig. 5: Examples of photo-TPs of SPX (from Engler et al., 1998; Hubicka et al., 2013)

In contrast to their high photoreactivity, FQs have shown low degradation rates through other abiotic processes like hydrolysis (Li & Zhang, 2010; Łukaszewicz et al., 2016; Wang et al., 2017).

While the emergence of largely unknown photo-TPs is considered an environmental risk factor due to their potentially differing and damaging characteristics (Arsand et al., 2018; Ledakowicz et al., 2019), their formation is used for the "Benign by Design" concept. The approach targets the problem of environmentally persistent pharmaceuticals and aims at developing compounds which combine improved biodegradability after the intended use with retained or improved pharmacological properties (Kümmerer, 2007). Through photodegradation, a non-targeted derivatisation of the compounds can be conducted which leads to the formation of a variety of photo-TPs with potentially differing biodegradability. The TPs displaying improved biodegradability can subsequently be tested for their pharmacological activity by applying quantitative structure-activity relationships (QSAR) prediction models and molecular docking. Consequently, the developed pharmaceuticals are less environmentally harmful, because they are not persistent and contribute less to the problems of toxicity and resistances through continuous exposure (Klatte et al., 2017; Leder et al., 2015). With the approach becoming more acknowledged during recent years, there are already several examples for successful application. Research performed on antineoplastics showed that the biodegradability of the non-degradable cancer drug ifosfamide could be improved by adding a glucose moiety to the molecular structure (Kümmerer & Al-Ahmad, 1997; Kümmerer et al., 2000b). The method of untargeted derivatisation through photolysis was applied to the β-blocker metoprolol. Here, the photodegradation process led to a number of TPs showing improved biodegradability while possibly retaining their pharmacological activity. However, some of the promising candidates showed signs of mutagenicity (Rastogi

et al., 2014). With the aforementioned problem of rising bacteria resistances to antibiotics, current research also targets the development of alternative antibiotics displaying improved degradability characteristics in the environment (Leder et al., 2018).

To induce the degradation and derivatisation, several methods such as the (photo-)Fenton process, oxidation through applying ozone and the irradiation with UV light exist (Real et al., 2010; Trovó et al., 2008). The method of UV irradiation, which was applied in this thesis, constitutes a safe and efficient way to achieve the formation of photo-TPs. UV radiation and especially UVC radiation with wavelengths below 280 nm is absorbed by most pharmaceuticals and can therefore decrease the concentration of the substances (Kawabata et al., 2013). The favoured reaction caused by exposure to UV light is the homolysis of bindings, leading to the formation of radicals. These radicals can either react with each other or with solute oxygen in the solvent, resulting in the formation of peroxyl and oxyl radicals and further degradation reactions (Heit et al., 1998).

2.3. Biodegradation

In the aquatic environment, organic substances can be degraded or transformed by microorganisms equipped with the corresponding enzymes. During dissimilation processes, substances are modified through biodeterioration, which includes the oxidation of organic substances under oxygen consumption. These processes can lead to detoxification (through e.g. hydroxylation, dehalogenation or methylation) or to activation (through e.g. hydrolysis of esters) of the initial compound (Alexander, 1999). Assimilation leads to the growth of biomass by utilisation of the organic substance as a source of carbon. When an organic substance can be degraded completely to inorganic substances (e.g. H_2O, CO_2), it is mineralised. Biodegradation processes can be separated into different phases: In the acclimation period, only a very slight degradation (up to 10%) is detected while the microorganisms adapt to the substrate. This is followed by the degradation phase in which an exponential growth of the microorganisms leads to the maximum possible level of degradation. In the subsequent plateau phase no significant change of the degradation level occurs. The time lengths of these phases are subject to major variation, depending on the substrate, the microorganisms and the surrounding conditions. Additionally, potential antimicrobial effects of the substrate should be considered (Alexander, 1999).

The biodegradability of substances is of high relevance for their environmental assessment. Substances which cannot or only very slowly be degraded are more persistent and can therefore unfold their potentially damaging, e.g. toxic, characteristics over longer periods of

time. While all researched FQs have proved to not be readily biodegradable, some studies have stated a certain level of inherent biodegradability (see table 2). In these cases, research has also targeted the identification of resulting bio-TPs which can differ in their ecotoxicity and residual antibiotic activity (Čvančarová et al., 2015; Jia et al., 2019; Maia et al., 2014). When discussing antibiotics, the persistence of substances contributes to the aforementioned problem of resistant bacteria. Spontaneous mutations causing resistances are fostered. These selection pressures can already arise at low environmental concentrations. (Martin-Laurent et al., 2019). Due to this relevance, biodegradability is frequently determined experimentally, according to multiple test methods established by OECD guidelines. To test for ready biodegradability in an aqueous medium, the DOC Die-Away Test, CO_2 Evolution Test, MITI (I)-Test, CBT, Modified OECD Screening Test and Manometric Respirometry Test are applied. On account of its applicability for poorly soluble, volatile and adsorbing compounds as well as the possibility of non-invasive measurements, the CBT was applied in this thesis (Friedrich, 2010; OECD, 1992a). The ZWT was conducted to test for inherent biodegradability and is usually applied if substances have been researched to not be readily biodegradable (OECD, 1992b).

Tab. 2: Biodegradability of various FQs

Substance	*Biodegradability [%]*	*Inoculum*	*Reference*
Ciprofloxacin, Ofloxacin	0	Effluent WWTP Freiburg	Kümmerer et al., 2000
Levofloxacin, Marbofloxacin	0	Effluent WWTP, Activated sludge	Bergheim et al., 2015
Sarafloxacin	8	Activated sludge	Bergheim et al., 2015
Ciprofloxacin	32	Activated sludge	Li & Zhang, 2010
Levofloxacin	52	Activated sludge	Maia et al., 2016
Ofloxacin	58	Activated sludge	Maia et al., 2016

2.3.1. Closed Bottle Test

The principle of the CBT was specified by the OECD in July 1992 under guideline 301 D. During the CBT, the test substances are incubated in the dark with a mineral medium and the effluent of a WWTP for 28 days under aerobic conditions. Respirometry is used as the analytical method to determine the level of dissolved oxygen. The substrate is the only source of carbon for the microorganisms and can potentially be oxidised through their activity. By comparing the oxygen decrease to the theoretical oxygen demand (ThOD) necessary for complete mineralisation, the degree of degradation can be calculated. In addition to the test bottles, a toxicity control is employed to test for antimicrobial effects of the substance and

avoid falsely negative results. To correct the results with the oxygen decrease caused by substrate present in the medium, a blank bottle without substance is incubated as well. A quality control is employed to test the activity of the microorganisms with a reference substance which is known to be readily biodegradable. Reference compounds, which are applied in the quality and toxicity controls, can be sodium acetate, sodium benzoate or freshly distilled aniline. For a substance to be considered readily biodegradable, a degradation increase from 10 to 60% must be achieved within 10 days (OECD, 1992a).

2.3.2. Zahn-Wellens Test

The current version of the ZWT was adopted by the OECD guideline 302 B in 1992 and was modified from the original version adopted in 1981. The test substances are agitated and aerated with mineral nutrients and activated sludge from a WWTP in an aqueous medium for 28 days at 20–25 °C, avoiding direct light. Biodegradation is determined by measuring the decrease of DOC which equals the degradation level. This test method is suitable for non-volatile and water-soluble compounds which should not significantly adsorb, get lost by foaming or inhibit bacteria at the concentration tested. High concentrations of substance (50–400 mg DOC L^{-1}) can increase the analytical reliability. Similar to the CBT, a blank value, a quality control and toxicity controls are applied. Ethylene glycol, diethylene glycol (DEG), lauryl sulfonate and aniline can be used as reference substances and should reach degradation levels of at least 70% within 14 days to ensure the validity of the test. Physiochemical adsorption of the test substances can play a role and is indicated by substantial substance removal during the first 3 h. To draw a more precise distinction between biodegradation and adsorption, further respirometric tests can be carried out. If very low values of degradation occur, the possibility of inhibition should be ruled out (OECD, 1992b).

3. Materials and Methodology

3.1. Required Instruments and Reagents

Tab. 3: Required instruments

Instrument	*Type*	*Manufacturer*
Analytical balance	ENTRIS224I-1S	Sartorius
PH electrode	SenTix® 41	WTW
Photoreactor	800 mL	Costum-made
UV lamp	Medium pressure, TQ 150	Heraeus
Syringes	Injekt® solo, 10 mL, Luer	B. Braun
PES filters	CHROMAFIL® Xtra PES-45/25; pore size 0.45 µm, filter-Ø 25 mm	Macherey-Nagel

TOC analyser	TOC-V_{CPN}, autosampler ASI-V	Shimadzu
HPLC	• Liquid chromatograph LC-20AT • UV/VIS-detector SPD-20AV • Auto sampler SIL-20AC HT • Column oven CTO-20AC • Diode array detector SPD-M20A • Communication module CBM-20A	Shimadzu
HPLC software	LabSolutions Version 5.54	Shimadzu
HPLC column	EC 150/2 Nucleoshell PFP, 2.7 µm	Macherey-Nagel
COD cell test	Spectroquant®, 5–80 mg L^{-1}, model CSB01796, lot number HC873121	Merck Millipore
Photometer	PhotoLab S12	WTW
Thermoreactor	CR 3000	WTW
Fibox 3 system	–	PreSens
Sensorspots	–	PreSens

Tab. 4: Required reagents

Reagent	*CAS number*	*Purity [%]*	*Manufacturer*
SPX	110871-86-8	≥ 99	Sigma Aldrich
1M sulphuric acid	7664-93-9	–	Carl Roth
Formic acid (0.1%) in water	64-18-6	≥ 98	Merck
Acetonitrile	75-05-8	≥ 99.9	VWR
DEG	111-46-6	≥ 99	Carl Roth
Sodium azide	26628-22-8	≥ 99	Sigma Aldrich
1M sodium hydroxide	1310-73-2	–	Carl Roth
Sodium acetate	127-09-3	≥ 99	Sigma Aldrich
Solution A (8.50 g L^{-1} KH_2PO_4, 21.75 g L^{-1} K_2HPO_4, 33.40 g L^{-1} $Na_2HPO_4 \cdot 2\ H_2O$, 0.50 g L^{-1} NH_4Cl)	KH_2PO_4: 7778-77-0 K_2HPO_4: 7758-11-4 $Na_2HPO_4 \cdot 2\ H_2O$: 10028-24-7 NH_4Cl: 12125-02-9	KH_2PO_4: ≥ 99 K_2HPO_4: ≥ 99 $Na_2HPO_4 \cdot 2\ H_2O$: ≥ 98 NH_4Cl: ≥ 99.5	KH_2PO_4: Carl Roth K_2HPO_4: Carl Roth $Na_2HPO_4 \cdot 2\ H_2O$: Fluka Analytical NH_4Cl: Carl Roth
Solution B (36.4 g L^{-1} $CaCl_2 \cdot 2\ H_2O$)	10035-04-8	≥ 99	Carl Roth
Solution C (22.5 g L^{-1} $MgSO_4 \cdot 7\ H_2O$)	10034-99-8	≥ 99	Carl Roth
Solution D (0.25 g L^{-1} $FeCl_3 \cdot 6\ H_2O$)	10025-77-1	≥ 97	Carl Roth
Sewage sludge	–	–	–
Effluent of WWTP	–	–	–

3.2. Photodegradation of Sparfloxacin

The photodegradation experiments were performed with a medium pressure UV lamp once for an irradiation time of 256 min and once for 496 min to determine the optimal endpoints for the biodegradation assays.

The stock solution was prepared by weighing in 250 mg of SPX and placing it in a 1 L volumetric flask. The flask was filled up with ultrapure water. After placing the flask on a magnetic stirrer and adding a stirring bar, the pH value was measured and set to a value of 3 by adding several drops of 1M sulphuric acid. Then, the flask was placed in an ultrasonic bath until the substance had dissolved completely.

Of the three exits of the photoreactor, one was closed, a tap was placed in the right exit and a pH electrode in the left exit (picture of reactor in figure 8). The reactor was rinsed and filled up with 800 mL of the stock solution. Underneath the fume hood, the UV lamp was placed in the reactor and the reactor with a stirring bar on the magnetic stirrer on a high level. The cooling was turned on and a stopper was placed in the upper exit.

Samples were taken at the times of 0, 2, 4, 8, 16, 32, 64, 128 and 256 min, and for the irradiation of 496 min additionally at 316, 376, 436 and 496 min. For each sampling, the stopper was taken out of the upper exit and 1 mL of the solution was let out of the tap and discarded. Then, 7 mL of the solution were filled into a centrifuge tube and the stopper was replaced. The samples were filtered into TOC vials using syringes and polyether sulfone (PES) filters and 1 mL of the samples was transferred to HPLC vials. The temperature and pH value were noted for each sampling time. After taking the 0 min sample, the UV lamp was turned on.

3.3. DOC and HPLC Measurement

The samples were diluted with ultrapure water (3 mL sample, 3 mL ultrapure water) and the DOC was measured. For the HPLC analysis, an existent method from the institute was applied and adapted to fit the experimental setting. A HPLC column with 150 mm length, 2 mm diameter and 2.7 µm particle size was used. The flow rate was 0.3 mL min^{-1}, with a column temperature of 45 °C and an injection volume of 10 µL for the photolysis and 100 µL for the biodegradation samples. The substances were measured with a UV detector at 254 and 300 nm and with a PDA detector at 230–600 nm. Acetonitrile and 0.1% formic acid in water were used as solvents with a gradient. From 0–2 min, the share of acetonitrile was 5%, from 2–25 min 35% and from 25–33 min 5%.

Following these measurements, the solutions of SPX irradiated with UV light for 0 min (SPX_0), 128 min (SPX_{128}) and 256 min (SPX_{256}) were chosen as optimal times for the biodegradation assays. Criteria for this choice were a preferably large number and peak area of TPs and a high degree of SPX degradation in the photolysis solutions. These solutions were then produced with a volume of 2 L each and the DOC was measured. Based on the HPLC results, the rate constant k, half-life $t_{0.5}$ and lifetime τ were calculated for the photodegradation of SPX by applying equations [1]–[3].

$$k\left[\text{min}^{-1}\right] = \ln\frac{\text{initial concentration } c_0}{\text{concentration at point in time t } c_t} \cdot \frac{1}{t\ [\text{min}]} \quad [1]$$

$$t_{0.5}\ [\text{min}] = \frac{\ln 2}{k\left[\text{min}^{-1}\right]} \quad [2]$$

$$\tau\ [\text{min}] = \frac{1}{k\left[\text{min}^{-1}\right]} \quad [3]$$

3.4. Closed Bottle Test

SPX_{128} and SPX_{256} were diluted 1:11 and their absorbance was measured using the test kit, photometer and thermoreactor. The measured mean values of 1.6585 (SPX_{128}) and 1.6450 (SPX_{256}) were converted to the chemical oxygen demand (COD) through the calibration curve depicted in figure 6. The correction with the measured water absorbance of 2.19 led to COD values of 332.19 mg L^{-1} (SPX_{128}) and 338.50 mg L^{-1} (SPX_{256}).

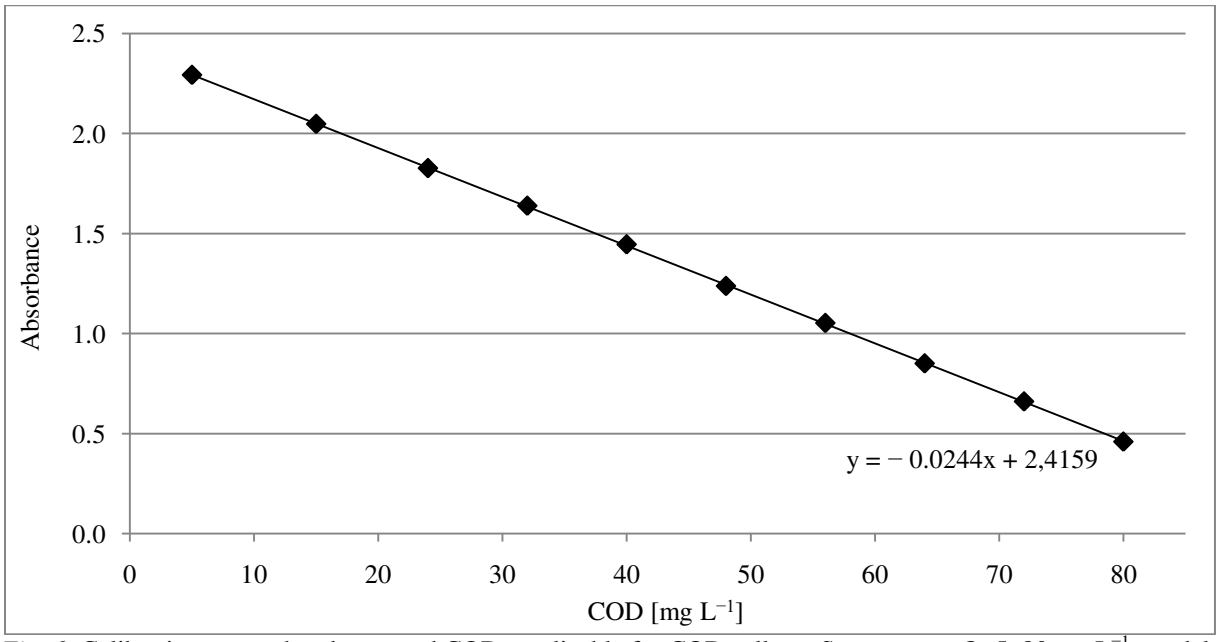

Fig. 6: Calibration curve absorbance and COD, applicable for COD cell test Spectroquant®, 5–80 mg L^{-1}, model CSB01796, lot number HC873121

A sodium acetate solution was prepared by dissolving 320 mg sodium acetate in 250 mL ultrapure water. 10 mL of the prefabricated solutions A–D were added to 10 L distilled water in the order B, C, D, A and the canister was shaken before adding solution A. The effluent of the WWTP was taken from the WWTP in Lüneburg (Abwasser, Grün und Lüneburger Service GmbH, 325000 eq. inhabitants) on the day of the test setup. The effluent was filtered through a paper filter, the first 200 mL were discarded and then, 20 drops were added to the distilled water to prepare the medium. The pH value was adjusted to 7.4 by adding several drops of 1M sodium hydroxide.

For each of the chosen times (SPX_0, SPX_{128} and SPX_{256}), a test and a toxicity control (Tox) were prepared in Schott flasks. Additionally, a blank value (BV) and a quality control (QC) were prepared. The substances were added according to table 5, leading to a ThOD of 5 mg L^{-1} in the tests and the QC and 10 mg L^{-1} in the toxicity controls. The volume of added substances was calculated by equation [4].

$$V_{substance}\ [mL] = \frac{\text{target ThOD}\ [mg\ L^{-1}]}{\text{current ThOD of substance}\ [mg\ L^{-1}]} \cdot V_{test\ bottle}\ [1000\ mL] \qquad [4]$$

The pH value of the Schott flasks was measured and two narrow neck bottles with sensor spot and stirring bar were filled from each Schott flask to perform all tests in duplicate. An additional narrow neck bottle without sensor spot was filled with distilled water as a temperature bottle. The bottles were closed and incubated in the dark at 20 °C for 28 days.

Tab. 5: Substances added in the CBT

	Medium [mL]	*Substance [mL]*	*Sodium acetate sol. [mL]*
BV	1000	–	–
QC	995	–	5
SPX_0	987.4	12.6	–
SPX_0 Tox	982.4	12.6	5
SPX_{128}	984.9	15.1	–
SPX_{128} Tox	979.9	15.1	5
SPX_{256}	985.2	14.8	–
SPX_{256} Tox	980.2	14.8	5

The oxygen concentration was measured non-invasively with the Fibox 3 system on days 0, 1, 2, 3, 6, 7, 9, 10, 13, 14, 15, 16, 17, 20, 21, 22, 23, 24, 27 and 28. For each measurement, the temperature sensor was placed in the temperature bottle. Then, the narrow neck bottles were placed on the magnetic stirrer and the fiber optic oxygen sensor was held to the middle of the sensor spot until 10 measurement points were taken in the plateau phase. The biological

oxygen demand (BOD) was determined by equation [5] and the percentage of degradation was calculated by equation [6].

$$\text{BOD [mg O}_2\text{ mg}^{-1}\text{ test substance]} = \frac{\text{mg O}_2\text{ L}^{-1}\text{ uptake by test substance} - \text{mg O}_2\text{ L}^{-1}\text{ uptake by blank}}{\text{mg test substance L}^{-1}\text{ in vessel}} \quad [5]$$

$$\text{Degradation [\%]} = \frac{\text{BOD [mg O}_2\text{ mg}^{-1}\text{ test substance]}}{\text{ThOD [mg O}_2\text{ mg}^{-1}\text{ test substance]}} \cdot 100 \quad [6]$$

On days 0 and 28, 1 mL HPLC samples were taken and stored at − 20 °C until HPLC analysis with the previously described method and an injection volume of 100 µL was conducted.

3.5. Zahn-Wellens Test

A DEG and a sodium azide solution were prepared by dissolving 2 g sodium azide and 1.1097 g (1 mL) DEG in 50 mL ultrapure water each. The activated sewage sludge was taken from the WWTP in Lüneburg (Abwasser, Grün und Lüneburger Service GmbH, 325000 eq. inhabitants) on the day of the test setup. Prior to use, the sludge was washed three times with tap water and centrifuged at 1000 rpm for 5 min.

Erlenmeyer flasks were set up on the magnetic stirrers with stirring bars underneath the fume hood, according to figure 7. Graduated pipettes of 1 or 2 mL volume were inserted through the holes in the stoppers. For each of the chosen times (SPX_0, SPX_{128} and SPX_{256}), two tests (a and b) and one toxicity control (Tox) were prepared in the Erlenmeyer flasks. Additionally, one flask contained the blank value (BV) und another one the quality control (QC). In Schott flasks, one sterile control (St) per chosen time was prepared by adding sodium azide to avoid aerobic degradation. All flasks were filled up with the substances according to table 6, leading to a DOC concentration of 50 mg L^{-1} in the tests and 100 mg L^{-1} in the toxicity controls respectively. The volume of the added substances was calculated by equation [7], using the DOC measurements of 133.0 mg L^{-1} (SPX_{128}) and 134.1 mg L^{-1} (SPX_{256}).

$$V_{\text{substance}}\,[\text{mL}] = \frac{\text{target DOC concentration}\,\left[\text{mg L}^{-1}\right]}{\text{current DOC concentration of substance}\,\left[\text{mg L}^{-1}\right]} \cdot V_{\text{test bottle}}\,[1000\text{ mL}] \quad [7]$$

The prefabricated solutions A–D were added in the order B, C, D, A and the sludge was added last, with a concentration of 1 g L^{-1} dry matter. The magnetic stirrers were switched on to a low level and the flasks were ventilated with CO_2-free compressed air through the pipettes. The sterile controls were closed and placed underneath the fume hood as well. The test ran for 28 days.

Tab. 6: Substances added in the ZWT

	Dist. H_20 [mL]	*Sludge [mL]*	*Sol. A [mL]*	*Sol. B [mL]*	*Sol. C [mL]*	*Sol. D [mL]*	*DEG sol. [mL]*	*Sub-stance [mL]*	*NaN_3 sol. [mL]*
BV	679.3	307.7	10	1	1	1	–	–	–
QC	674.3	307.7	10	1	1	1	5	–	–
SPX_0 a & b	335.4	307.7	10	1	1	1	–	343.9	–
SPX_0 St	635.1	–	10	1	1	1	–	343.9	8
SPX_0 Tox	330.4	307.7	10	1	1	1	5	343.9	–
SPX_{128} a & b	303.4	307.7	10	1	1	1	–	375.9	–
SPX_{128} St	603.1	–	10	1	1	1	–	375.9	8
SPX_{128} Tox	298.4	307.7	10	1	1	1	5	375.9	–
SPX_{256} a & b	306.3	307.7	10	1	1	1	–	373.0	–
SPX_{256} St	606.0	–	10	1	1	1	–	373.0	8
SPX_{256} Tox	301.3	307.7	10	1	1	1	5	373.0	–

Samples were taken at 0 days, 3 h, 1 day, 3, 7, 10, 14, 17, 21, 24 and 28 days. At 3 h, no samples were taken from the sterile controls. On day 1, the liquid level was marked on the vessels after taking the samples. On all following days, the vessels were filled up to that mark with distilled water. The pH value was measured and set to 7.2–7.4 with 1M sodium hydroxide and 1M sulphuric acid. 7 mL samples were taken out of the vessels und filtered into TOC Vials using syringes and PES filters. The DOC was measured for all samples and the degradation was calculated by equation [8], taking the 3 h measurements as a start value. Additionally, the degradation in the test bottles and the toxicity controls was calculated with the theoretical DOC as a start value by applying equation [9] (see discussion).

Degradation [%] =

$$(1 - \frac{\text{DOC in test at time t } \left[\text{mg L}^{-1}\right] - \text{DOC in BV at time t } \left[\text{mg L}^{-1}\right]}{\text{DOC in test after 3 h } \left[\text{mg L}^{-1}\right] - \text{DOC in BV after 3 h } \left[\text{mg L}^{-1}\right]}) \cdot 100 \qquad [8]$$

Degradation [%] =

$$(1 - \frac{\text{DOC in test at time t } \left[\text{mg L}^{-1}\right] - \text{DOC in BV at time t } \left[\text{mg L}^{-1}\right]}{\text{theoretical DOC } \left[\text{mg L}^{-1}\right]}) \cdot 100 \qquad [9]$$

1 mL of the samples was transferred to HPLC vials and stored at − 20 °C until HPLC analysis.

Fig. 7: Setup ZWT

4. Results and Discussion

4.1. Photodegradation of Sparfloxacin

When mixed with water, SPX formed a bright yellow solution. The substance dissolved completely after setting the pH value to 3 and applying the ultrasonic bath for a few minutes. After 30 min of exposure to UV light, the solution started to darken until it reached a mixture between brown and red after approximately 128 min (see figure 8). Afterwards, no visible change in colour occurred. This colour change from yellow to brown/red indicates that the formed substances absorb light of longer wavelengths. With non-bonding orbitals absorbing longer wavelengths (Elbert & Logue, 1999), it can therefore be assumed that the electron system of the initial substance was expanded, e.g. by adding groups containing oxygen.


Fig. 8: SPX solution after 128 min (left) and 256 min (right) of photolysis

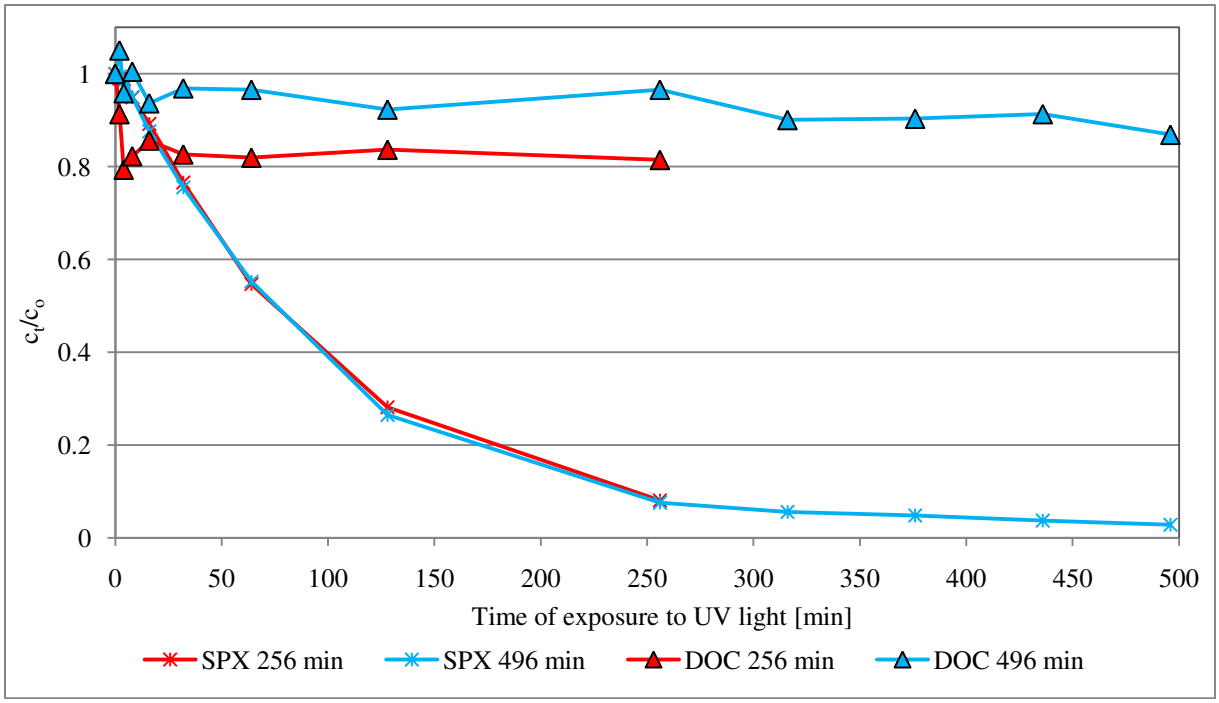

Fig. 9: SPX and DOC development during 256 min (red) and 496 min (blue) irradiation with UV light

In figure 9, the development of SPX (measured by peak area) and DOC over the time of UV irradiation is depicted. The recovery rate of the calculated DOC value was 97.03% for the 256 min photolysis and 84.52% for the 496 min photolysis. While a decrease of SPX over time could be observed, the DOC concentration remained relatively stable with values staying above 80% of the initial concentration.

The decrease of SPX peak area during irradiation indicates that SPX was degraded by exposure to UV light. When considering the absorbance spectrum of SPX depicted in figure 10 and the emittance spectrum of the UV lamp in figure 11, major overlaps of these spectra are visible. It can therefore be assumed that SPX was mainly influenced by direct photolysis, because the substance could absorb the UV light itself. Further indirect photolysis reactions through formation of e.g. oxyl radicals and the resulting oxidation reactions could have accelerated the process. However, the photolysis did not depend on these, since the emitted wavelengths could be directly absorbed by SPX.

When plotting the logarithmical peak area against the time, a linear decrease was achieved, thus characterising the photodegradation kinetics of SPX as a first-order reaction. For the irradiation of 496 min, a rate constant of $k = 7.8 \cdot 10^{-3}$ min^{-1}, a half-life of $t_{0.5} = 88.87$ min and a lifetime of $\tau = 128.21$ min were determined for SPX under the given conditions. This finding corresponds with the results by Hubicka et al. (2013), confirming a first-order reaction for the photodegradation of SPX by UVA radiation. However, the degradation in these experiments occurred significantly faster than described by Hubicka et al. (2013) with a rate constant of $12.3 \cdot 10^{-3}$ h^{-1} and a half-life of 56.34 h. Due to Hubicka et al.'s (2013) use of

UVA irradiation with wavelengths of 320–400 nm, the light was absorbed substantially less by SPX, as the optimal wavelength of 298 nm was not emitted. With the second smaller peak at 371 nm (see figure 10), SPX could still partly absorb the emitted UVA light and was degraded, but these reactions took place at a substantially slower rate.

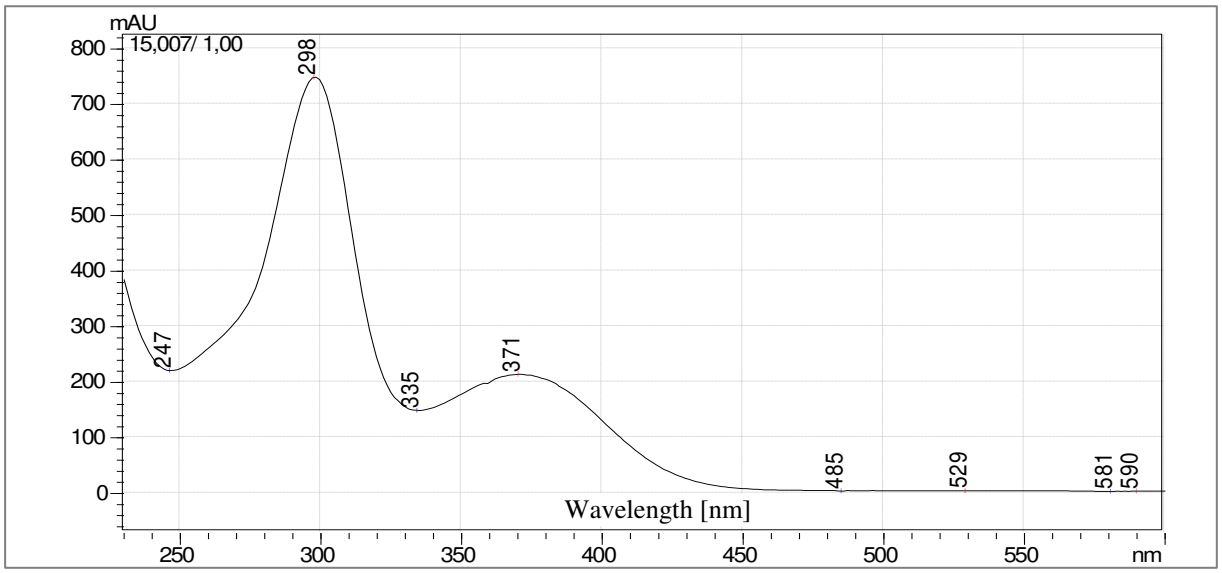

Fig. 10: Absorbance spectrum of SPX, measured with PDA detector, 230–600 nm

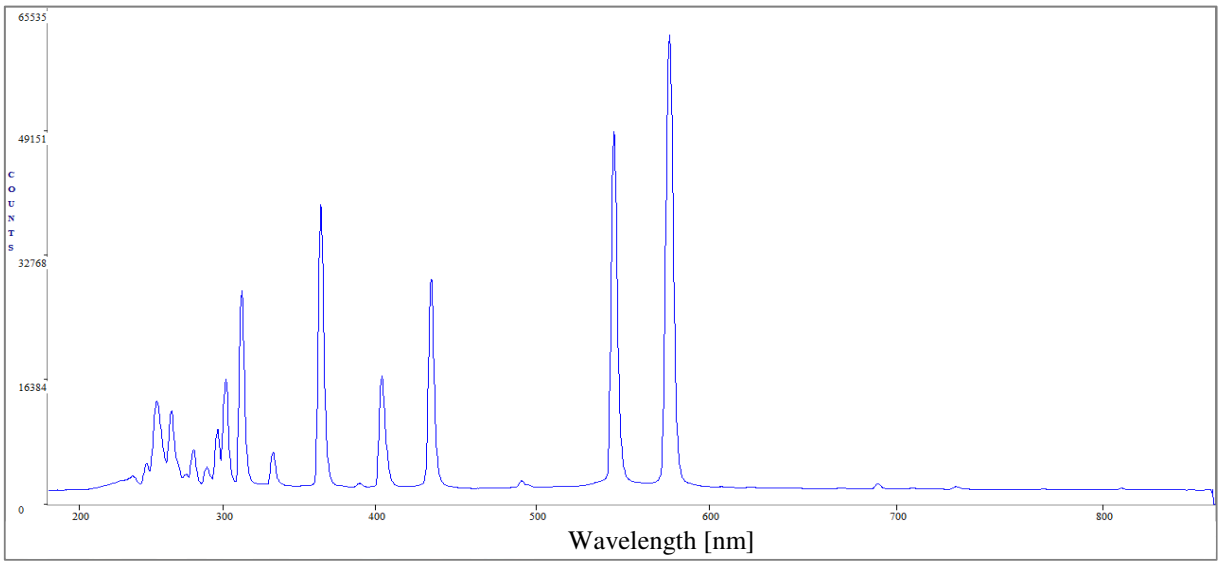

Fig. 11: Emittance spectrum of the applied medium pressure UV lamp, type TQ 150, from Heraeus, Germany

Furthermore, with FQs being ionisable substances, the photodegradation kinetics are influenced significantly by the pH value. FQs in the cationic form have been researched to display the lowest quantum yield and therefore slowest degradation rates, while the quantum yield was highest in slightly alkaline solutions (Wammer et al., 2013). It can therefore be assumed that photodegradation would occur even faster at a higher pH value.

The merely slight decrease of the DOC during the irradiation time indicates that the major share of degraded SPX was not mineralised to inorganic substances, but converted to TPs which developed through the irradiation. Similar results have been achieved in

photodegradation experiments with other FQs where mineralisation was slower than the degradation of the FQs, due to the emerging TPs contributing to the DOC (e.g. Li et al., 2012). The slight decrease in the beginning and fluctuations of the DOC can be explained by measurement inaccuracies as well as substances getting caught on the filter.

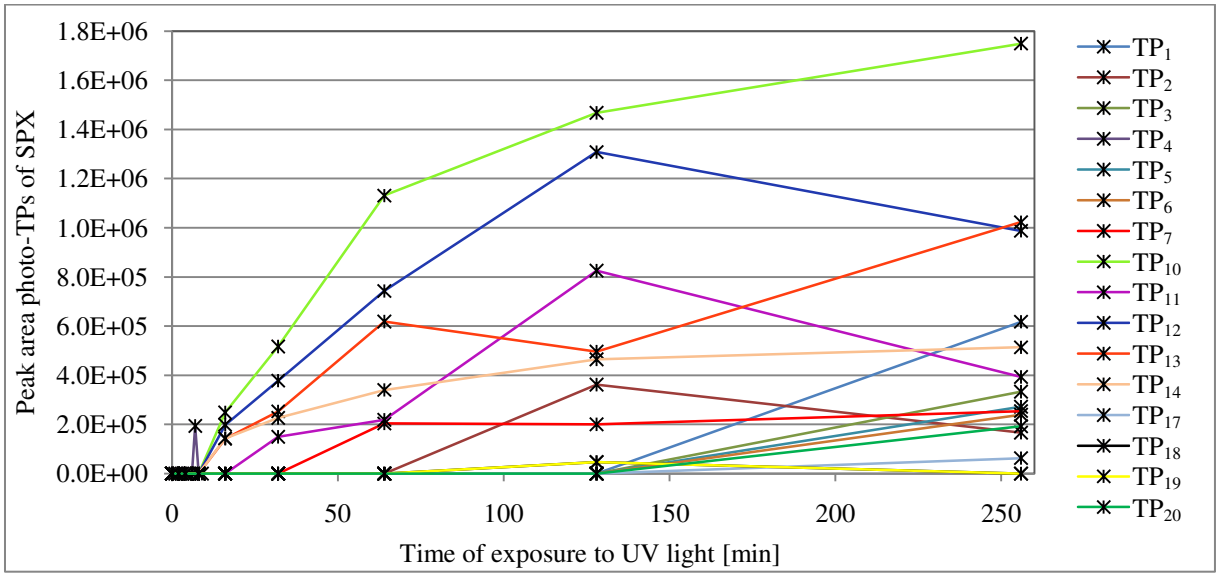

Fig. 12: Development of photo-TPs SPX during 256 min irradiation with UV light

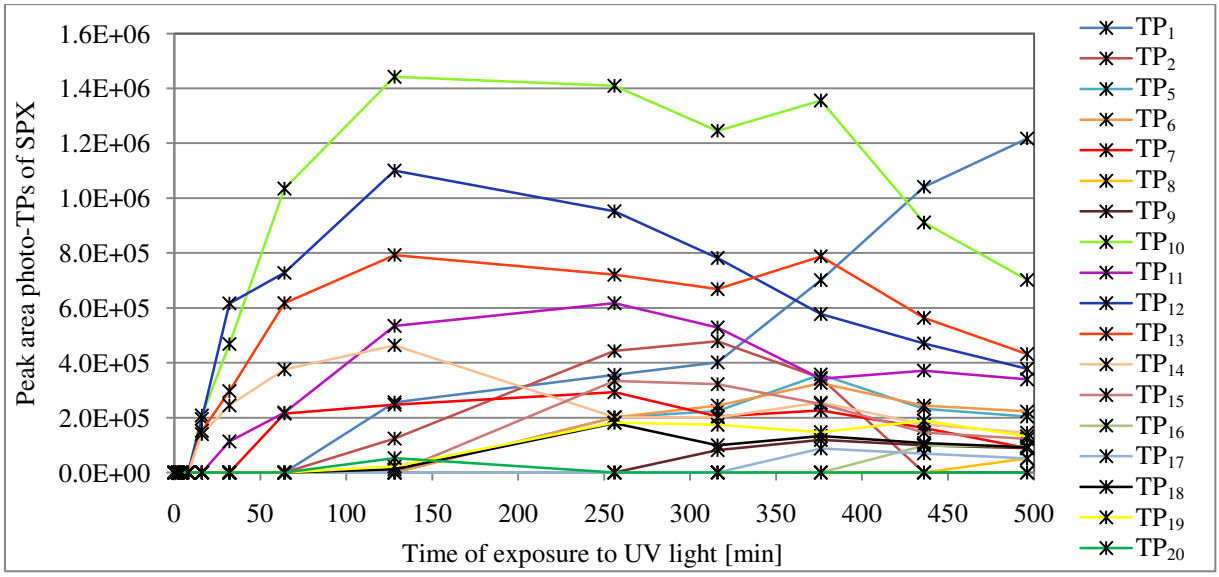

Fig. 13: Development of photo-TPs SPX during 496 min irradiation with UV light

Through HPLC analysis of the photolysis solutions, 20 different photo-TPs were detected. The TPs were numbered according to their retention times (retention times and wavelengths for measurements can be found in annex A). Figures 12 and 13 show the development of these TPs during 256 (figure 12) and 496 (figure 13) min of irradiation with UV light. Of these 20 TPs, 17 had a shorter retention time than SPX and were therefore more polar substances, while 3 TPs showed longer retention times, identifying them as less polar substances. In figure 13, it can be observed that most TPs reached their maximum peak area at the measurements of 128 and 256 min and were decreasing afterwards, with few exceptions

(especially TP_1). Due to these optima of TP peak area in combination with the high degradation level of SPX at these times (see figure 9), the irradiation solutions of 128 and 256 min were chosen as points in time to test for biodegradability. This matches the findings by Engler et al. (1998), stating an optimal irradiation time of 4 h to establish TPs of SPX through UV light. While UV irradiation was only carried out for 8 h at the most in these experiments, the SPX peak area reached a nearly constant size towards the end of the exposure time, in accordance with the results by Engler et al. (1998).

Due to the limited extent of this thesis, no isolation and identification of the arising TPs was conducted. When considering the findings by Hubicka et al. (2013), identifying seven more polar and two less polar TPs through mass spectrometry, it can be assumed that these previously identified TPs and a number of constitutional isomers were present in the photolysis solutions created in these experiments. The most common structural changes included the replacement of fluorine and amine substituents with hydroxyl groups on the nucleus and the addition of functional groups to the piperazine substituent (Hubicka et al., 2013; see figure 5).

4.2. Closed Bottle Test

4.2.1. Biodegradation Closed Bottle Test Determined by O_2 Consumption

The mean degradation values of the QC, test substances and toxicity controls over time are depicted in figure 14 with indicated standard deviations. The QC reached 24 ± 1.2% of degradation after 28 days, SPX_0 reached a value of − 4 ± 1.4% and the photolysis solutions were degraded by 3 ± 2.8% (SPX_{128}) and 4 ± 1.4% (SPX_{256}). The degradation of the toxicity controls was measured between 43 ± 0.6% and 36 ± 0.4%, with SPX_{256} reaching the highest level of degradation.

The conducted test fulfilled the validity criteria of the oxygen consumption in the BV being lower than 1.5 mg L^{-1} on day 28 and the oxygen concentration in the tests being above 0.5 mg L^{-1}. Furthermore, the differences of extremes of replicate values were less than 20% and the degradation of the toxicity controls was above 25% on day 28. However, the validity criterion of the QC being degraded by at least 60% on day 14 was not fulfilled (OECD, 1992a). Considering the toxicity controls, in which sodium acetate as a reference substance was substantially degraded, the test can still be regarded as valid. The low degradation of the QC was likely caused by a mistake in the conduction of the experiment, for example by adding not enough volume of the sodium acetate solution.

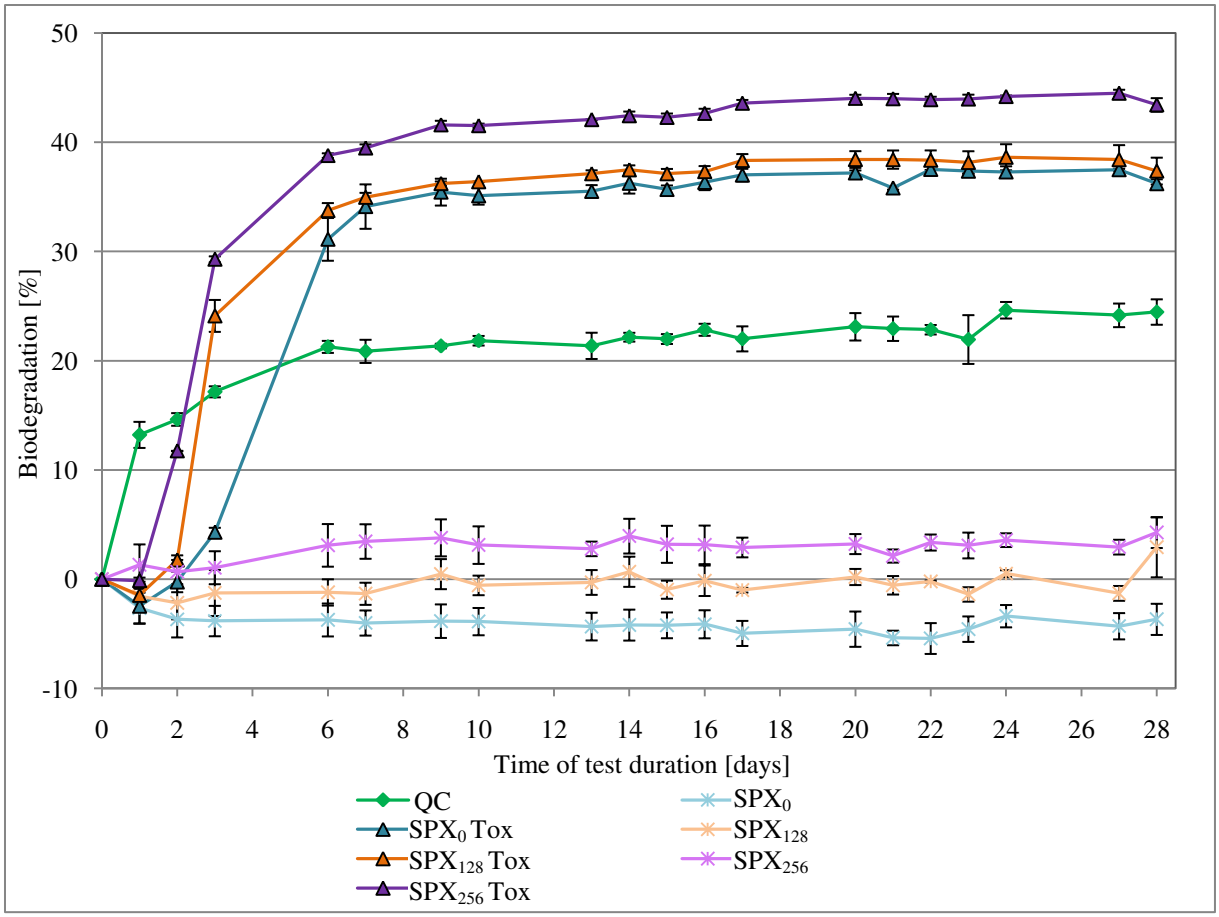

Fig. 14: Biodegradation of test substances, toxicity controls and QC during CBT over test duration of 28 days

With none of the test substances reaching the defined degradation level of 60%, both the SPX and the photolysis solutions were not readily biodegradable (OECD, 1992a).

The negative values in SPX_0 can be interpreted as 0% degradation and arose from the subtraction of the O_2 uptake in the BV, which was higher than in the test bottles due to the toxicity of SPX. With SPX concentrations exceeding the MIC values (table 1), the substances displayed toxicity as expected. When comparing the toxicity controls, it can be observed that the inhibition by the SPX solutions was decreased through photolysis. This is shown by the shorter inhibition time at the start of the test, as well as by the overall achieved higher degradation in the toxicity controls of the photolysis solutions. This decrease of toxicity increased with the time of UV irradiation, with SPX_{256} showing the lowest level of toxicity. Lower toxic effects on bacterial strains through UV irradiation have also been stated for other FQs, such as levofloxacin, marbofloxacin and sarafloxacin (Bergheim et al., 2015). Lower acute toxicity of organic substances often results from reductive or oxidative dehalogenation (Bunge & Lechner, 2009; Tominaga et al., 2018). When considering the identified TPs of SPX (figure 5), defluorination can be observed while hydroxyl and carbonyl groups were added. It can therefore be assumed that the decrease in acute toxicity was a result of oxidative defluorination. However, it should be noted that while the acute ecotoxicity decreased, the

TPs might still be able to spread resistance if they contain the same pharmacophores as the initial substance. In addition to this, no statements about chronic or human toxicity can be made.

4.2.2. Biodegradation Closed Bottle Test Determined by HPLC Analysis

The following figures show the results from the HPLC analysis of the solutions on day 0 and day 28 of the CBT. Mean values of the test bottles and the corresponding toxicity controls are depicted and the standard deviations are indicated. In figure 15, the measured SPX peak areas are displayed, while figure 16 shows the TPs in SPX_{128} and figure 17 in SPX_{256}. In the photolysis solutions, 22 different TPs were detected and numbered in order of their retention times (retention times and wavelengths of measurements in annex A). TP_1 to TP_{20} were more polar than SPX, while TP_{21} to TP_{23} were less polar. During the test period, the peak area of SPX remained nearly constant, no detectable new TPs emerged, and no TPs vanished. Only minor changes occurred in the peak area of some substances (e.g. slight increase TP_5, slight decrease TP_{13}). These minor changes indicate that neither SPX nor the arising TPs could be significantly degraded in any of the solutions during the CBT and are therefore not readily biodegradable. The small detected changes in peak area for some TPs can either result from bacterial activity or from measurement inaccuracies and are thus not sufficient to draw conclusions about which TPs to further investigate. These findings support the studies stating that FQs are generally not biodegradable, with research for example performed on ciprofloxacin, ofloxacin, levofloxacin and sarafloxacin (Bergheim et al., 2015; Kümmerer et al., 2000a).

While no studies on the ready biodegradability of photo-TPs arising from SPX were found, the results are in line with experiments conducted on the photo-TPs of ciprofloxacin (Vasconcelos et al., 2009) and ofloxacin (Vasquez et al., 2013). In both studies, the TPs were found to not be readily biodegradable when applying the CBT. When the test was performed with the TPs of ofloxacin, the ready biodegradability was improved by the presence of the secondary carbon source of sodium acetate, resulting in a higher degradation of the test substances in the toxicity controls. This degradability increase can potentially be explained by processes of cometabolism, as sodium acetate has been known to increase the biodegradability of several pharmaceuticals (Vasquez et al., 2013). However, this was not confirmed for the TPs of ciprofloxacin where the addition of sodium acetate did not lead to improved biodegradability in the CBT (Vasconcelos et al., 2009). In accordance with the results by Vasconcelos et al. (2009), the toxicity controls in this test did not differ

substantially from the test vessels. Thus, no indication for processes of cometabolism could be observed. Cometabolism in the presence of sodium acetate is still not fully understood and can be assumed to be substrate specific (Vasquez et al., 2013).

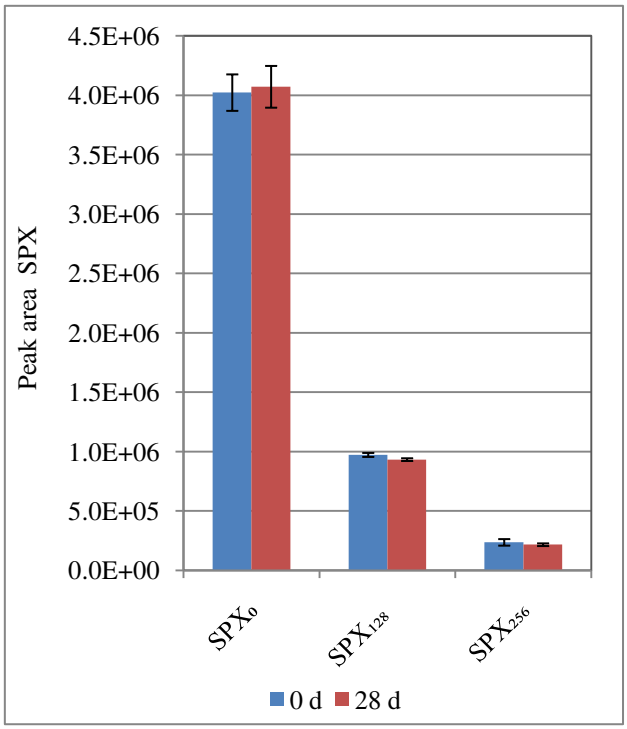

Fig. 15: SPX development during CBT; SPX peak areas of 0 (blue) and 28 (red) days measurements are depicted

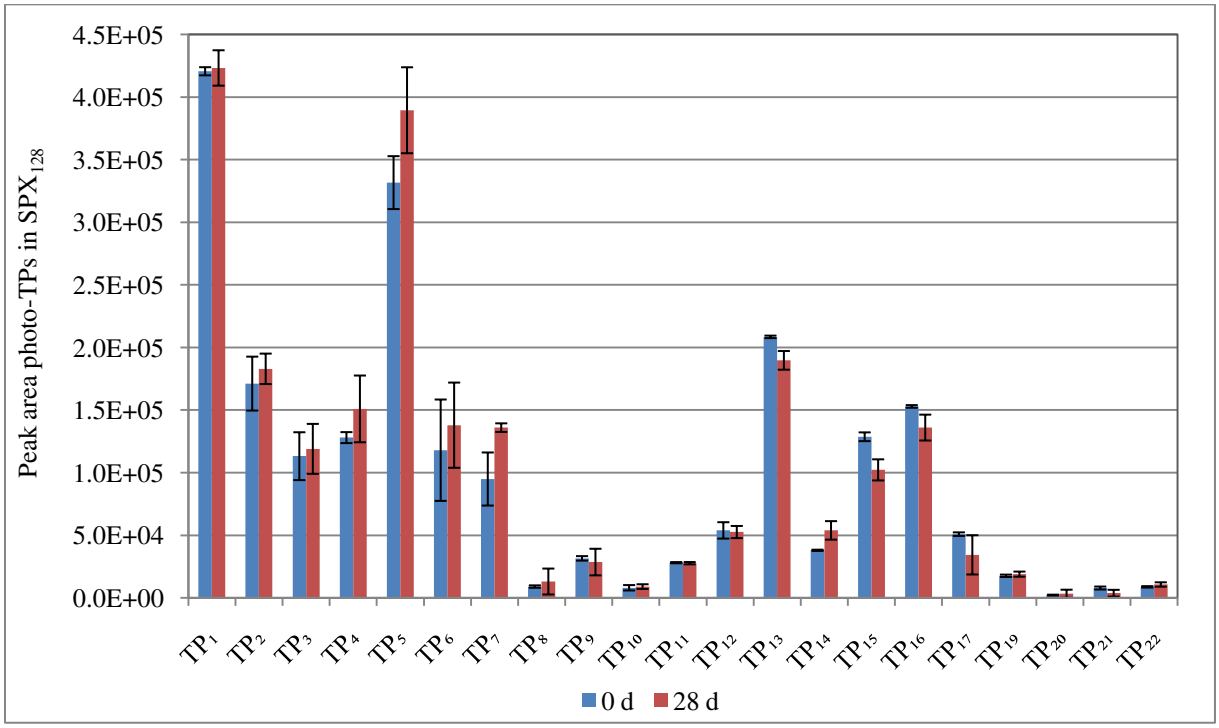

Fig. 16: Development of photo-TPs 1–22 in SPX_{128} during CBT; TP peak areas of 0 (blue) and 28 (red) days measurements are depicted

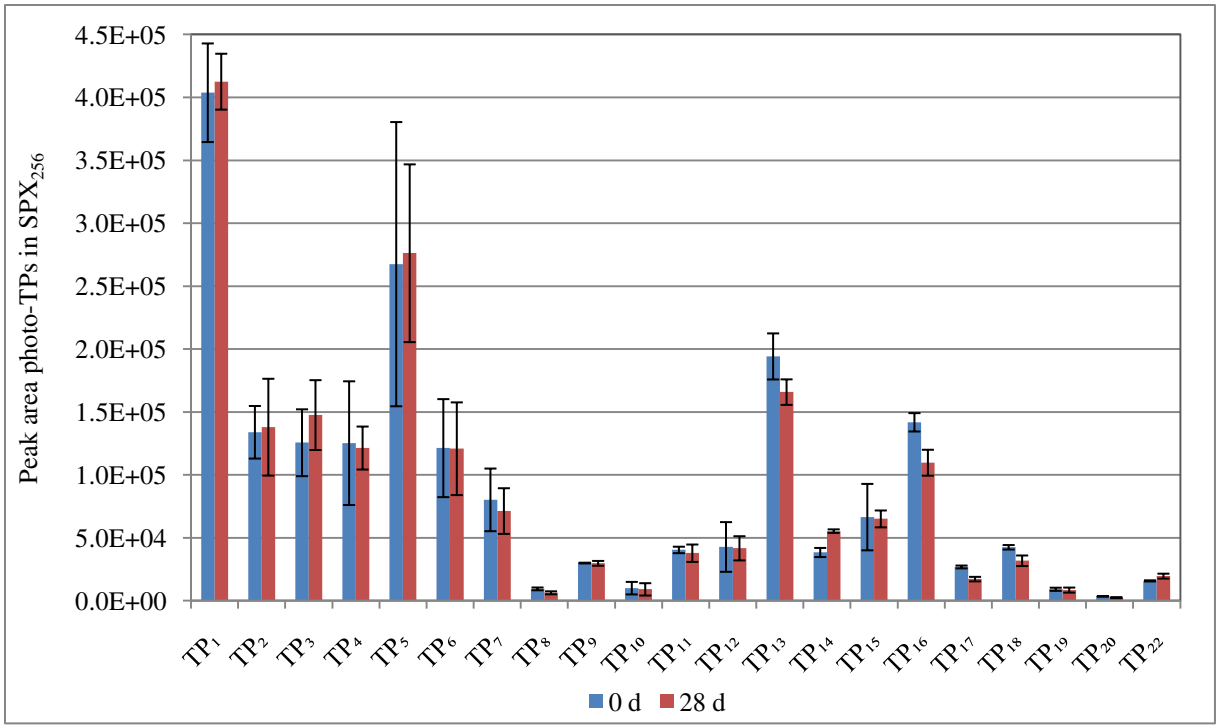

Fig. 17: Development of photo-TPs 1–22 in SPX_{256} during CBT; TP peak areas of 0 (blue) and 28 (red) days measurements are depicted

4.3. Zahn-Wellens Test

4.3.1. Degradation Zahn-Wellens Test Determined by DOC Measurement

Throughout the test duration, profuse foam formation was observed in all test bottles with activated sludge. The most foam was produced in the bottles containing SPX_0. It should be noted that the WWTP reported procedural problems during the sludge collection. These can potentially have caused the exceptionally profuse foaming.

Figure 18 shows the degradation of the QC, test substances, toxicity controls and sterile controls during the test duration of 28 days. Mean values and corresponding standard deviations are displayed for the test substances and the measurements of 3 h were taken as the start value. The QC was degraded by 97%. The test substances reached degradation values of − 33 ± 3.5% (SPX_0), − 37 ± 1.0% (SPX_{128}) and 4 ± 29.2% (SPX_{256}). During the test period, major variations of the measured degradation level were observed for all test substances. They reached negative values of up to − 85% and partly displayed high standard deviations. For the toxicity controls, a degradation between 67% and 58% was measured, with SPX_{256} reaching the highest value and the sterile controls reached degradation values between 19% and 11%.

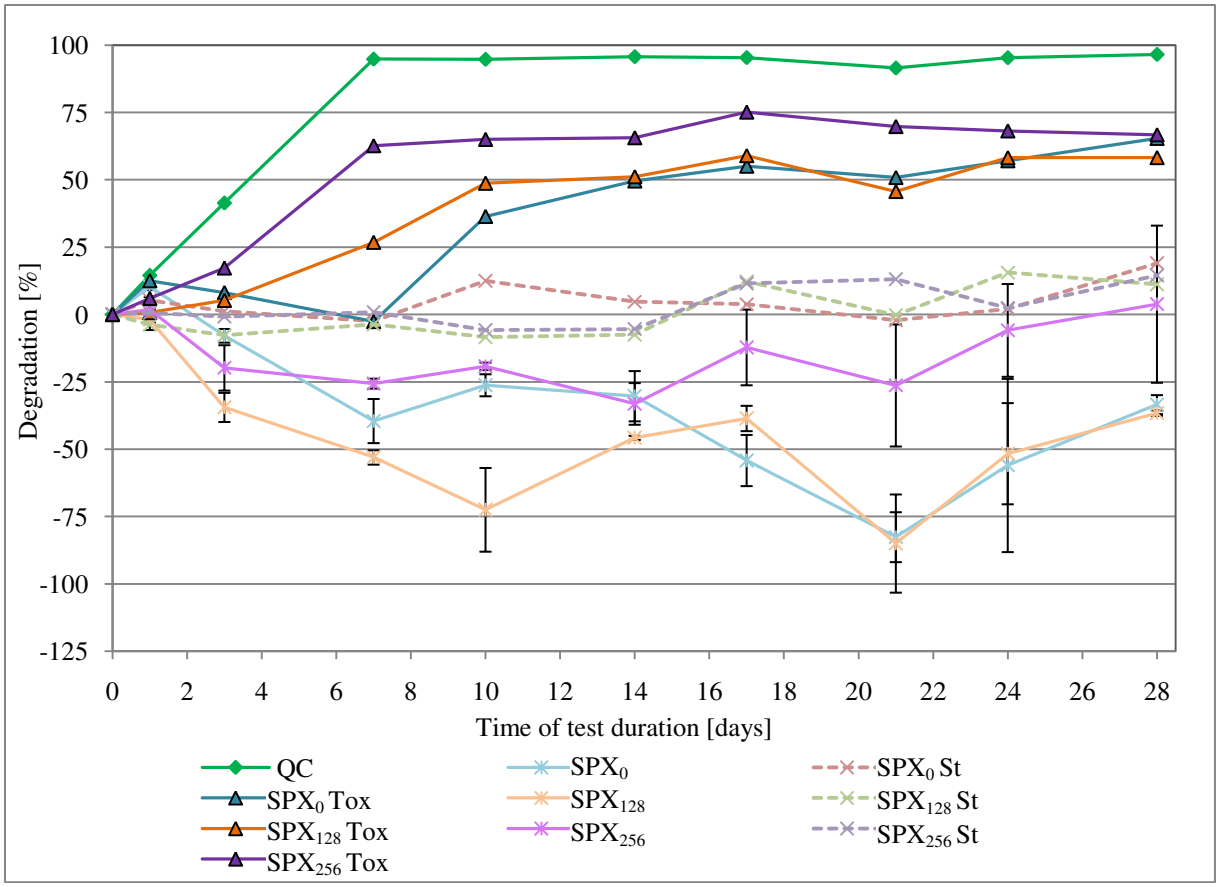

Fig. 18: Degradation of test substances, toxicity controls, sterile controls and QC during ZWT over test duration of 28 days; 3 h measurements taken as start value

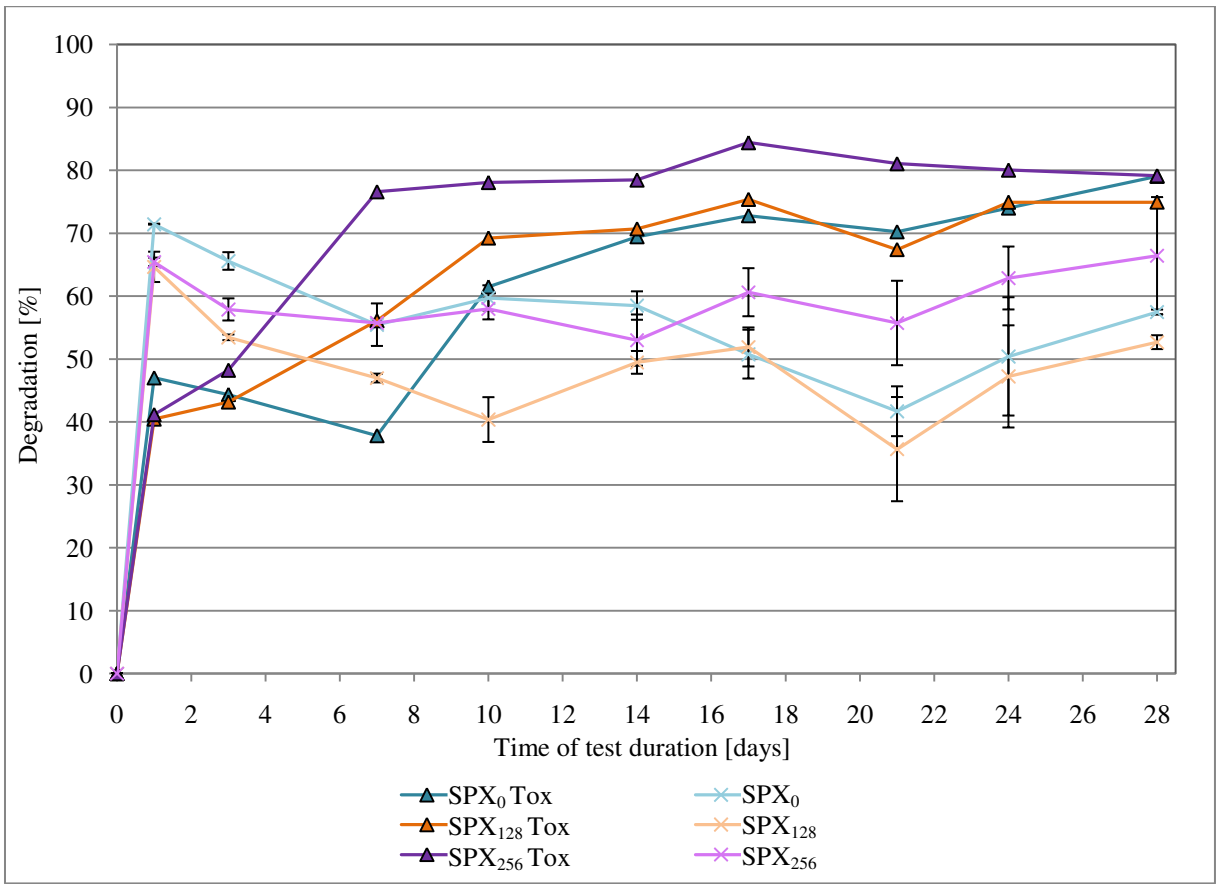

Fig. 19: Degradation of test substances and toxicity controls during ZWT over test duration of 28 days; theoretical DOC taken as start value

The test fulfilled the validity criterion of the reference substance DEG being degraded by at least 70% within 14 days (OECD, 1992b). For the reference substance, no adaptation phase could be observed. The biodegradation phase lasted 7 days until resulting in a constant degradation level in the plateau phase. With the test substances reaching negative or close to zero degradation levels, they cannot be considered inherently biodegradable from these test results. However, the validity criterion of the DOC removal in the test suspensions taking place relatively gradually over time was not fulfilled. Figure 18 shows substantial fluctuations in the degradation level as well as major differences between the degradation in test vessel a and b, indicated by high standard deviations.

FQs have been found to be subject to profuse adsorption to sewage sludge. The degree of adsorption depends on the pH value and the maximum adsorption arises at pH values between 6 and 8 (Zhou et al., 2013). While the pH value was set to a value of 7.2–7.4 prior to each sampling, acidification was observed between the samplings due to substances being transformed to the corresponding acids through oxidation, e.g. DEG to diglycolic acid (Landry et al., 2013). These fluctuations can be assumed to have influenced the degree of adsorption to the sewage sludge for SPX and its photo-TPs, leading to an alternation of desorption and adsorption depending on the current conditions. The fluctuations and negative degradation values can therefore assumed to not be the result of biodegradation, but of desorption and adsorption. While all toxicity controls reached relatively similar degradation levels at the end of the test, it can be observed that the photolysis solutions showed higher degradation throughout the test. This corresponds with the aforementioned results (section 4.2.1.) and the findings by Bergheim et al. (2015), stating that UV irradiation decreases the acute toxicity of FQs. While the degradation fluctuations were less profuse for the toxicity controls than for the test substances, it can be assumed that they were influenced by adsorption and desorption processes as well.

To achieve a better depiction of the degradation and adsorption processes, figure 19 shows the degradation of the test substances (mean values with displayed standard deviations) and the toxicity controls in the ZWT with the theoretical DOC concentration as a start value. It can be observed that for the test substances, a degradation between 71 ± 0.1% (SPX_0) and 65 ± 2.4% (SPX_{128}) occurred during the first day. While the degradation varied throughout the test period, it arrived at only slightly different levels at the end of the test. For the toxicity controls, a degradation between 47% (SPX_0) and 40% (SPX_{128}) was observed during the first day, with degradation levels increasing to values between 79% (SPX_{256}) and 75% (SPX_{128}) until the end of the test.

When considering this depiction, it can be observed that in the test vessels an adsorption of 65–71% of the test substances occurred in the beginning of the test. These results are in line with the findings by Zhou et al. (2013), stating that 50–72% of the amount of substance of various studied FQs adsorbed on sewage sludge. After this adsorption, fluctuations were observed, but no steady degradation could be detected. For the toxicity controls, the initial adsorption was significantly lower due to the presence of not only the test substances, but DEG as a reference substance as well, which does not adsorb substantially. For both the test vessels and the toxicity controls, SPX_0 showed a slightly higher adsorption than the photolysis solutions. This indicates that the adsorbability can potentially be decreased by UV irradiation due to the increased polarity of most TPs. Summarising, it can be said that no biodegradability of the test substances could be detected, but these results cannot be considered reliable due to the influence of the adsorbability of the substances. Further statements about the possible biodegradation of substances require the HPLC analysis which is discussed in section 4.3.3.

However, the achieved results contribute to the environmental assessment of the test substances. During recent years, sewage sludge has been increasingly applied in agriculture. The sludge poses the potential of replacing fertilisers by providing nutrients to the plants and improving soil properties. At the same time, by recycling the sludge the challenge of disposal of large amounts of organic waste is avoided. Due to these advantages, the usage of sewage sludge has been considered to be contributive to a sustainable agriculture by some studies (e.g. Bhatt et al., 2015). In contrast to these advantages, problems arise from the contamination with heavy metals (Tervahauta et al., 2014) and organic substances, specifically those displaying toxicity (Thomaidi et al., 2016). Adsorbing compounds are usually lipophilic and are therefore subject to bioaccumulation in the food chain. The high determined adsorption potential for SPX and its TPs indicates that the substances contribute to this problem and the criticism concerning the application of sewage sludge in agriculture.

The sterile controls of all test substances only showed low levels of degradation with no noteworthy differences between SPX_0 and the photolysis solutions. Consequently, this indicates that hydrolysis as an abiotic degradation process is not of major relevance for the degradation of the researched substances. In studies performed on ciprofloxacin, ofloxacin and other FQs, hydrolysis was found to be negligible (Li & Zhang, 2010; Wang et al., 2017). Łukaszewicz et al. (2016) determined half-lives of more than one year for hydrolytic degradation processes of ciprofloxacin, norfloxacin and enrofloxacin in the aquatic environment. While slow degradation of FQs through abiotic processes is observed, it does not contribute substantially to their removal. Further results about the abiotic degradation of

specific substances can be gained from the HPLC analysis discussed in the following section 4.3.2.

4.3.2. Abiotic Degradation Zahn-Wellens Test Determined by HPLC Analysis

In the ZWT, 41 different TPs were detected and numbered in order of their retention times. 27 of these TPs were more polar than SPX and 14 TPs were less polar. The higher number of detected TPs compared to the CBT can be explained by the higher concentrations used in the ZWT in combination with similar injection volumes. Thus, a more sensitive detection was achieved.

As shown in figure 20, the SPX peak areas in SPX_{128} St and SPX_{256} St remained relatively stable and a slight decrease was observed in SPX_0 St. In SPX_0 St, only TP_{24} which was present in all SPX_0 solutions (discussion see section 4.3.3.2.) was detected. Figure 21 shows the TPs in SPX_{128} St and SPX_{256} St displaying a decrease throughout the test duration. In both sterile controls, these included TP_{11}, TP_{16}, TP_{27} and TP_{30}. Additionally, TP_8 decreased in SPX_{128} St, while TP_6, TP_9, TP_{25}, TP_{28} and TP_{29} were reduced in SPX_{256} St. A complete depiction of all TPs in the sterile controls can be found in annex B.

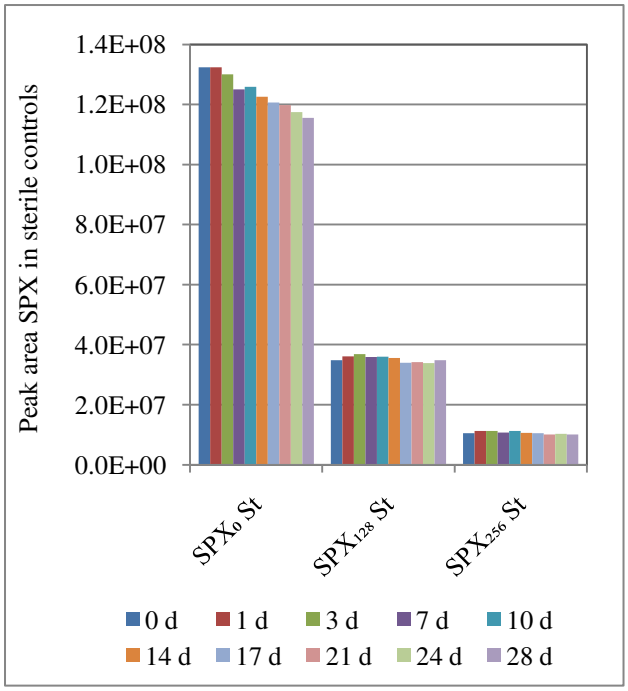

Fig. 20: SPX development in sterile controls during ZWT over test duration of 28 days

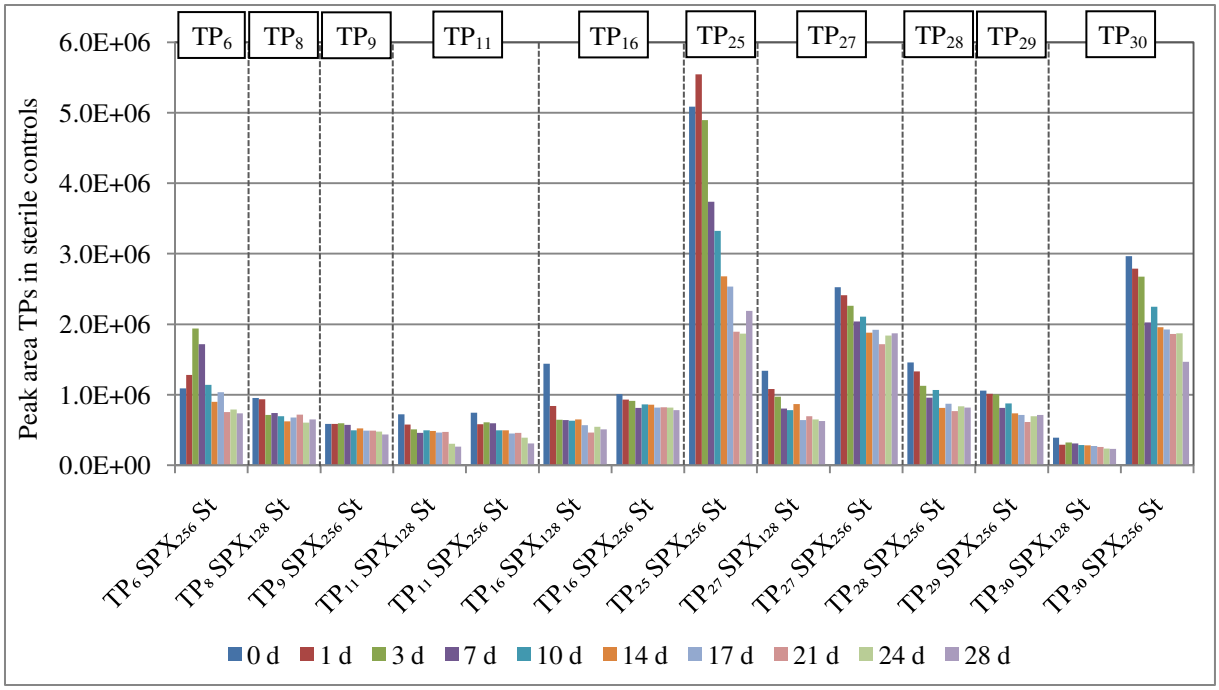

Fig. 21: Development of TPs decreasing in SPX_{128} St and SPX_{256} St during ZWT over test duration of 28 days

The slight decrease of SPX in SPX_0 St indicates that a slow degradation of SPX through abiotic degradation processes took place. Besides hydrolysis, reactions between SPX and sodium azide are possible, with FQs having already shown a certain reactivity with cyanide (Pan et al., 2014). However, this degradation was not observed in SPX_{128} St and SPX_{256} St. Hydrolysis reactions of organic compounds have been found to be dependent on the concentration of the compound, with the rate constant of hydrolysis decreasing with declining concentrations (Rathbun, 2000). It can therefore be assumed that the abiotic degradation of SPX was not detectable in SPX_{128} St and SPX_{256} St due to the lower concentrations. These low hydrolysis rates support the findings by Łukaszewicz et al. (2016) stating that the removal of FQs through abiotic degradation can only be achieved over long periods of time.

When considering the development of the TPs depicted in figure 21, it can be observed that several TPs displayed abiotic degradation rates exceeding the degradation of SPX, even though the corresponding peak areas were substantially smaller. During research performed on ciprofloxacin, the addition of a hemiaminal group led to the formation of a hydrolytically unstable compound (Leder et al., 2018). It can be assumed that the TPs of SPX displaying abiotic degradation had structures as proposed in figure 22. The structures either contain a hemiaminal group or act as strong reducing agents through hydroxyl groups in para or ortho positions. These TPs are of interest because the goal of eliminating the substance faster from the environment can not only be achieved through biotic, but also through abiotic degradation. Especially the TPs being degraded in both SPX_{128} St and SPX_{256} St show the potential for

improved abiotic degradation characteristics. An identification and further characterisation of these compounds could therefore be useful.

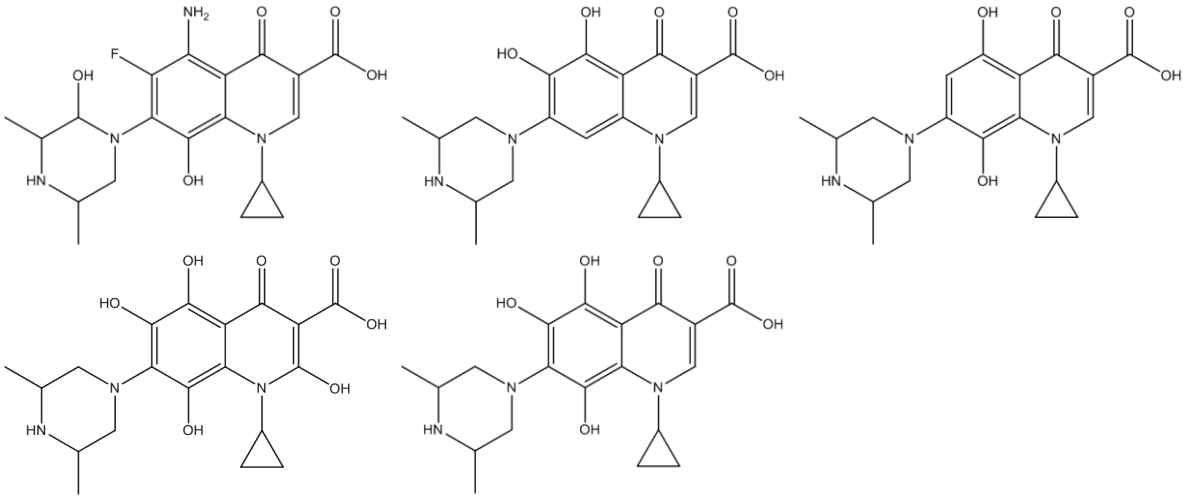

Fig. 22: Possible hydrolytically unstable and strong reducing TPs of SPX

4.3.3. Biodegradation Zahn-Wellens Test Determined by HPLC Analysis

In both the BV and the QC, two peaks with retention times of 1.93 and 2.55 min were detected after 3 days (see annex C). Therefore, these peaks were taken out of the results from SPX_0, where they also appeared after 3 days. In SPX_{128} and SPX_{256}, TP_1 and TP_2 with retention times of 1.98 and 2.66 min were present from the start of the test. Due to the very similar retention times and absorbance spectra, the peaks appearing in the BV and QC can be assumed to have fallen together with these already present TPs. However, solely through HPLC-DAD analysis no complete certainty that the arising compounds are the same as the ones already present through photodegradation can be established. Further analysis through mass spectrometry would be necessary to achieve a clear separation.

As previously mentioned, the substances were subject to major adsorption processes. The following analysis depicts the peak areas for all measurements including the samples taken at 0 days. To determine the development of compounds throughout the test, the 3 h measurements are used as a reference starting point. Furthermore, the pH dependent desorption and adsorption processes led to fluctuations in the concentrations of SPX and its TPs. Therefore, sudden fluctuations in the measured peak areas of the substances are treated as consequences of desorption and adsorption and are not included in the following discussion about the biodegradability of substances. Biodegradation or the emergence of bio-TPs is indicated by a gradual decrease or increase of the peak area of a substance (OECD, 1992b).

4.3.3.1. Development of SPX

As depicted in figure 23, the peak area of SPX in all test bottles and toxicity controls decreased during the test. Starting from day 3, until day 10 to 21, a slight increase in peak area was observed in all bottles, followed by a decrease towards the end of the test. The overall decrease of peak area was substantial for SPX_0 and SPX_{128}, with only a fraction of the initial peak area left at the end of the test. For SPX_{256}, the peak area only showed a slight decrease compared to the 3 h value.

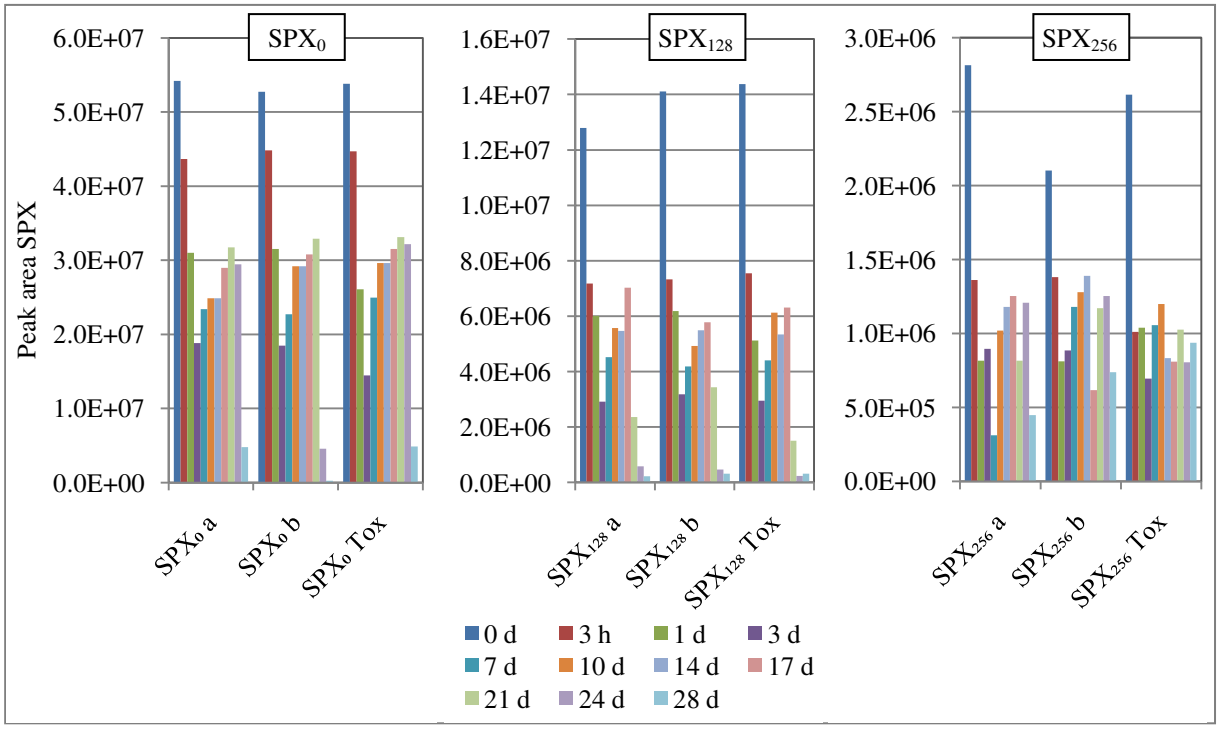

Fig. 23: SPX development in SPX_0, SPX_{128} and SPX_{256} during ZWT over test duration of 28 days

These results indicate that biodegradation was observed for SPX in SPX_0 and SPX_{128} during the ZWT, with the major degradation occurring within the last week of the test. While FQs have been researched to not be inherently biodegradable by several studies (e.g. Amorim et al., 2014), others stated a certain level of biodegradation (Li & Zhang, 2010; Maia et al., 2016). The differing results suggest that the inherent biodegradability depends on factors such as the concentration of the test substance, the different microbial communities present in the activated sludge and the experimental conditions like temperature and pH value. In comparison to SPX_0 and SPX_{128}, only minor biodegradation was observed in SPX_{256}. Considering that all solutions were incubated with the same microorganisms in the sludge under the same experimental conditions, this substantially lower degradation rate can be assumed to be caused by the lower initial concentration. During bacterial degradation, the enzymes responsible for the biotransformation of the compound must be activated. This is not evoked if the concentration of the substrate in the medium is lower than the necessary

threshold concentration (Maia et al., 2014). Another potential explanation is the presence of toxic TPs in SPX_{256} inhibiting those bacterial strains being able to degrade SPX in the other bottles. Processes of cometabolism in SPX_0 and SPX_{128} and competitive inhibition in SPX_{256} could have influenced the degradation as well. The fact that biodegradation was only observed towards the end of the test can potentially be explained by the high toxicity of SPX and its TPs. Consequently, just the resistant bacteria, which constituted only a small fraction of the microorganisms at the start of the test, were able to degrade the substance.

4.3.3.2. Development of Transformation Products in SPX_0

Throughout the test, six TPs were detected in the SPX_0 test bottles and the toxicity control, in addition to the peaks also arising in the BV. Figures 24 and 25 show the development of these TPs over time. While TP_{24} was present in all bottles from the start and experienced an increase followed by a decrease of its peak area, TP_{11}, TP_{21}, TP_{22}, TP_{27} and TP_{41} emerged at points in time between 17 and 28 days.

Even though this SPX solution was not exposed to UV light, TP_{24} was detected from the beginning of the test. With no appearance of this TP in the BV, it can be ruled out that the emergence was caused by substrate carried over in the activated sludge. It can be assumed that this TP was caused by an impurity of the SPX substance and was not detected in SPX_{128} and SPX_{256} because of its instability during UV irradiation.

All other TPs emerged throughout the test and can therefore be considered bio-TPs of SPX. While studies have targeted the bio-TPs arising from several FQs through incubation with mixed or isolated bacterial strains (e.g. Jia et al., 2019; Maia et al., 2014), no research has been performed concerning the identification of bio-TPs of SPX. Such an identification was neither performed as part of this thesis. Due to the similar initial molecule structure, it can be assumed that the resulting bio-TPs resemble the products identified by Jia et al. (2019) for the biotransformation of ciprofloxacin. Those products include structural changes arising from a cleavage of the piperazine substituent and hydroxylation (Jia et al., 2019). With most of the TPs significantly emerging during the measurements of 24 and 28 days, a clear connection to the decrease of SPX during the same measurements can be detected. It can therefore be assumed that TP_{11}, TP_{22}, TP_{27} and TP_{41} are direct bio-TPs of SPX, while no correlation between the decrease of SPX and the emergence of TP_{21} was observed. These bio-TPs are of interest for the environmental assessment of SPX because they may differ in their characteristics like toxicity and residual antibiotic activity (Čvančarová et al., 2015).

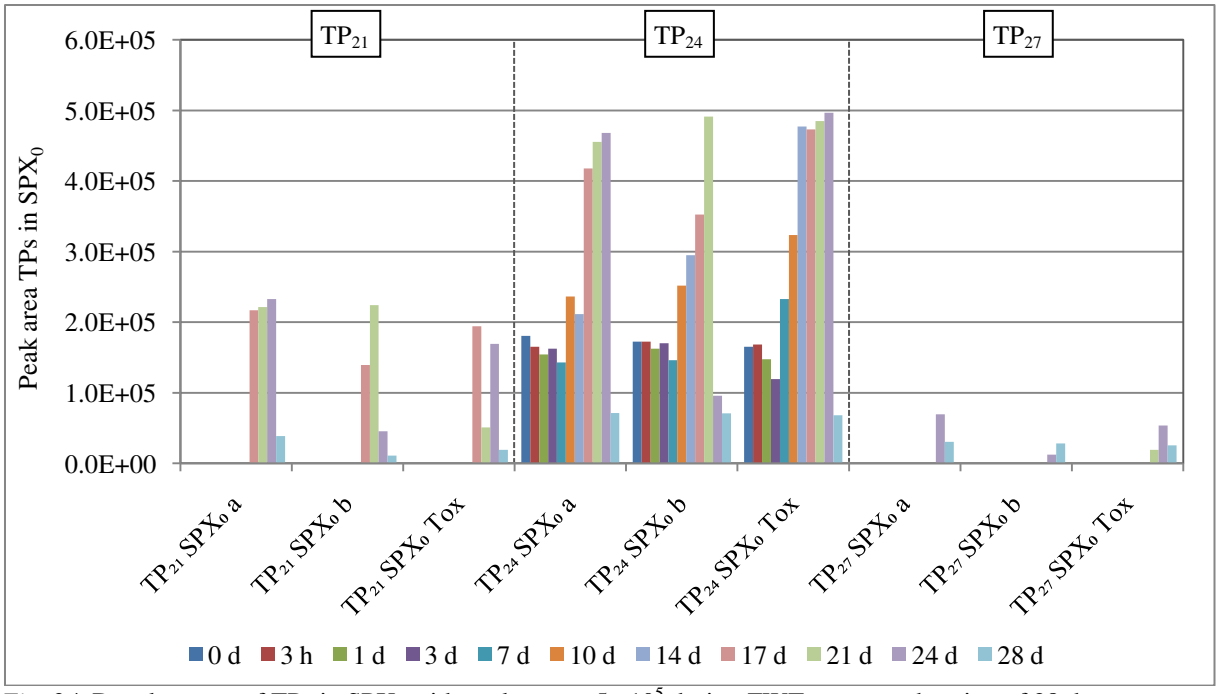

Fig. 24: Development of TPs in SPX_0 with peak area < $5 \cdot 10^5$ during ZWT over test duration of 28 days

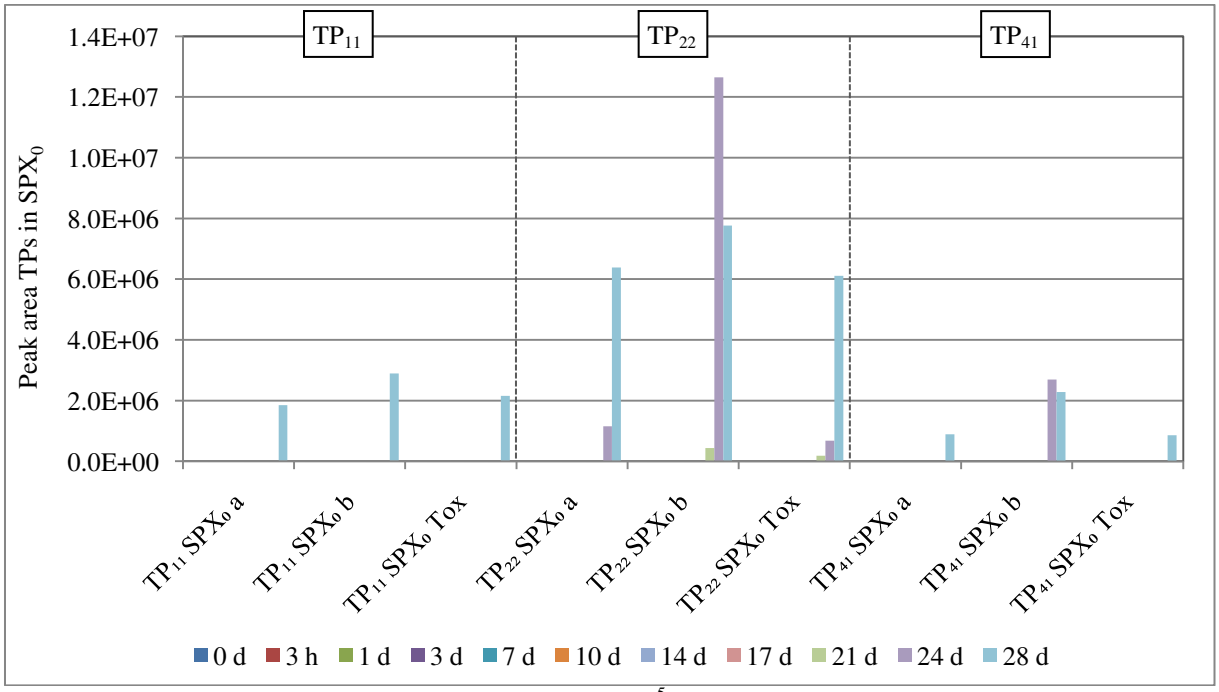

Fig. 25: Development of TPs in SPX_0 with peak area > $5 \cdot 10^5$ during ZWT over test duration of 28 days

4.3.3.3. Development of Relevant Transformation Products in SPX_{128} and SPX_{256}

The following results and discussion only include the relevant TPs from the SPX_{128} and SPX_{256} test bottles and toxicity controls. Criteria for considering a TP as relevant were newly emerging TPs, TPs with a notable change in peak area throughout the test duration and a general emphasis on TPs with higher intensity. The development of all TPs is depicted in annex D and E.

Five newly emerging TPs were detected as displayed in figure 26. TP_{15} and TP_{18}, which occurred at points in time between 14 and 17 days, were detected in all six bottles, with TP_{18} reaching larger peak areas in SPX_{128}. TP_{37}, TP_{40} and TP_{41} only occurred in SPX_{128} and all appeared at 24 days.

In accordance with the TPs arising from SPX_0, these newly emerging TPs can be considered bio-TPs (Maia et al., 2014). In the photolysis solutions, these bio-TPs can not only result from SPX, but also from the photo-TPs present in the solutions. To determine the degradation pathways, further analysis would be necessary. Considering that TP_{37}, TP_{40} and TP_{41} only emerged in SPX_{128} and at the same time as the major decrease of SPX was observed, these TPs can be assumed to be direct bio-TPs of SPX. The differences in peak area of TP_{18} between SPX_{128} and SPX_{256} can potentially be explained by differing concentrations of the biotransformation educts, competitive inhibition or processes of cometabolism. Besides the general relevance of bio-TPs, these TPs are of interest because their emergence indicates that a degradation of other substances takes place.

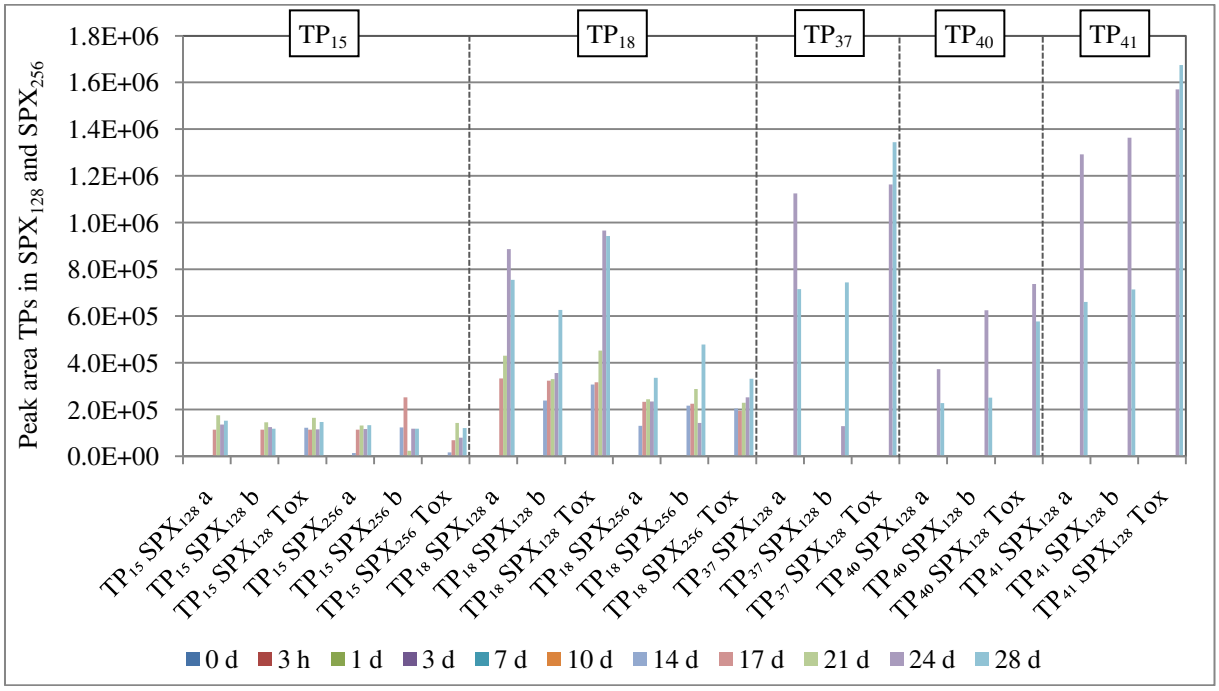

Fig. 26: Development of newly emerging TPs in SPX_{128} and SPX_{256} during ZWT over test duration of 28 days

During the test period, the peak areas of TP_1, TP_{11}, TP_{13}, TP_{22} and TP_{33} increased in the bottles with SPX_{128} and with SPX_{256}. Figure 27 shows the increasing TPs with peak areas $< 2 \cdot 10^6$. TP_1 showed a steady increase throughout the test, with slightly larger peak areas in SPX_{256}. For TP_{13}, the measured peak areas were larger in SPX_{128} and TP_{33} showed different levels of increase. Figure 28 depicts the increasing TPs reaching peak areas $> 2 \cdot 10^6$. For both TP_{11} and TP_{22}, the major increase which can be observed between days 21 and 28 in SPX_{128}

turned out considerably lower in SPX_{256}. In contrast to the test bottles, SPX_{256} Tox showed no increase in TP_{11}.

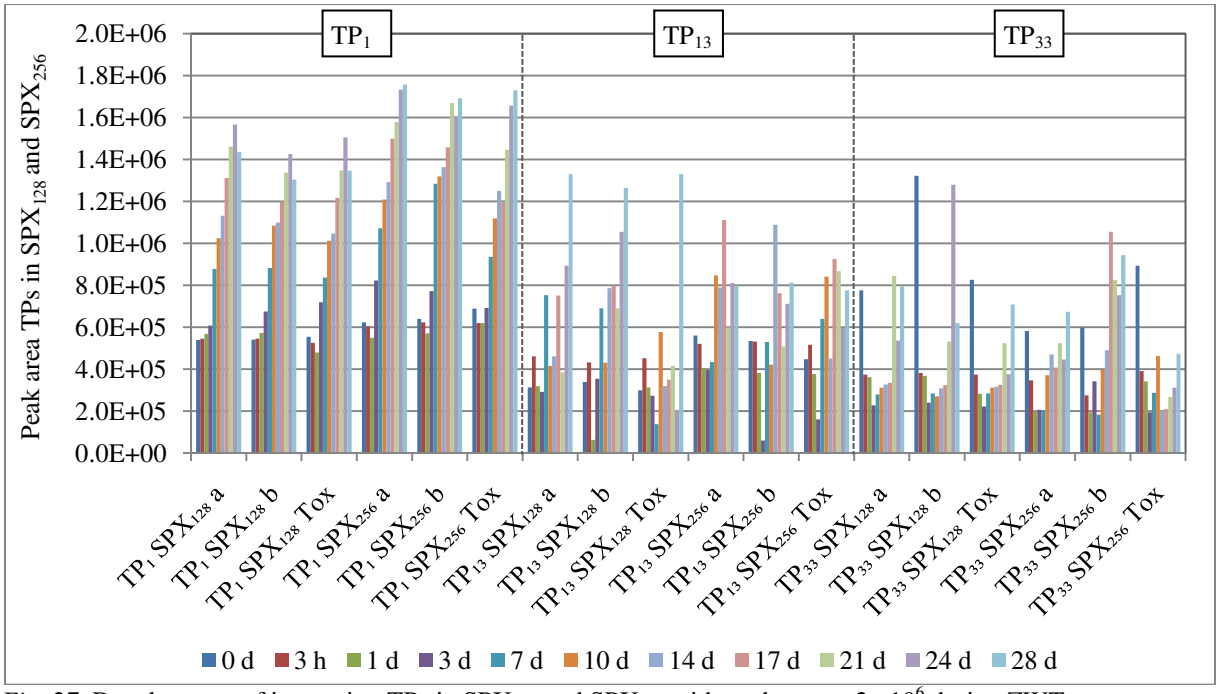

Fig. 27: Development of increasing TPs in SPX_{128} and SPX_{256} with peak area < $2 \cdot 10^6$ during ZWT over test duration of 28 days

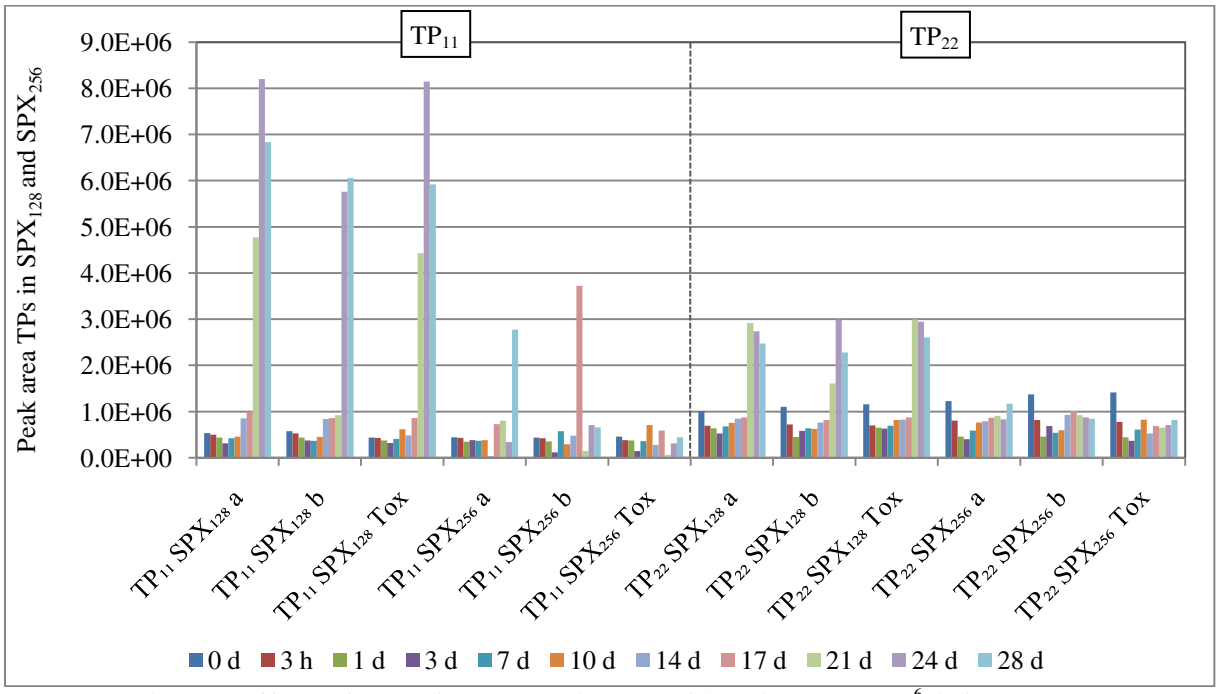

Fig. 28: Development of increasing TPs in SPX_{128} and SPX_{256} with peak area > $2 \cdot 10^6$ during ZWT over test duration of 28 days

In accordance with the newly emerging TPs, these increasing TPs are relevant because they indicate the emergence of bio-TPs and a decrease of other substances. Where the increase of TPs differed between the bottles, this can be explained by differing start concentrations of the compounds and a differing degree of the degradation of other substances. TP_{11} and TP_{22},

which displayed the most substantial increase in SPX_{128}, show a correlation with the decrease of SPX and can therefore be considered bio-TPs of SPX. No substantial decrease of SPX and therefore only a minor increase of the corresponding bio-TPs was observed in SPX_{256}. However, the detected higher peaks of TP_{11} on day 28 (test bottle a) and day 17 (test bottle b) also occurred at the same time as lower measured peak areas for SPX (see figure 28 and figure 23). Therefore, the lack of increase of TP_{11} in SPX_{256} Tox can be explained by the constant level of SPX peak area in this test bottle. With the microorganisms being able to degrade DEG as an energy supply in the toxicity control, there was less need to target other substances which were not as easily degradable.

Figures 29 and 30 depict the TPs showing a decrease during the test. These include TP_4, TP_{10}, and TP_{19} in both SPX_{128} and SPX_{256}. Additionally, in SPX_{128}, TP_3, TP_{24} and TP_{25} displayed a decrease, while in SPX_{256}, the peak area of TP_8 was reduced. At first, TP_3, TP_{24} and TP_{25} showed an increase in peak area before decreasing towards the end of the test. TP_4, TP_8, TP_{10} and TP_{19} displayed a decrease throughout the whole test, including some fluctuations. It can be noted that the major decrease between days 21 and 28 observed for the peak area of TP_{19} in SPX_{128} was not detected in SPX_{256}. Furthermore, the decrease of TP_4 was lower in SPX_{256}, with the SPX_{256} a test bottle showing no decrease at all.

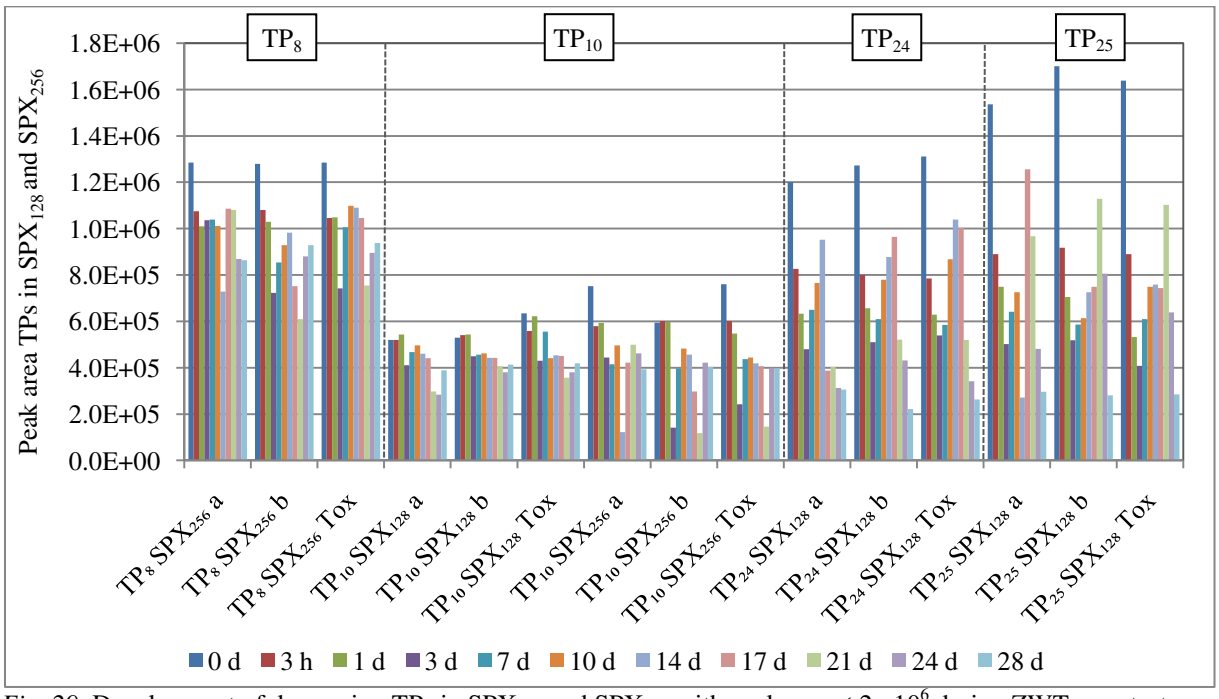

Fig. 29: Development of decreasing TPs in SPX_{128} and SPX_{256} with peak area < $2 \cdot 10^6$ during ZWT over test duration of 28 days

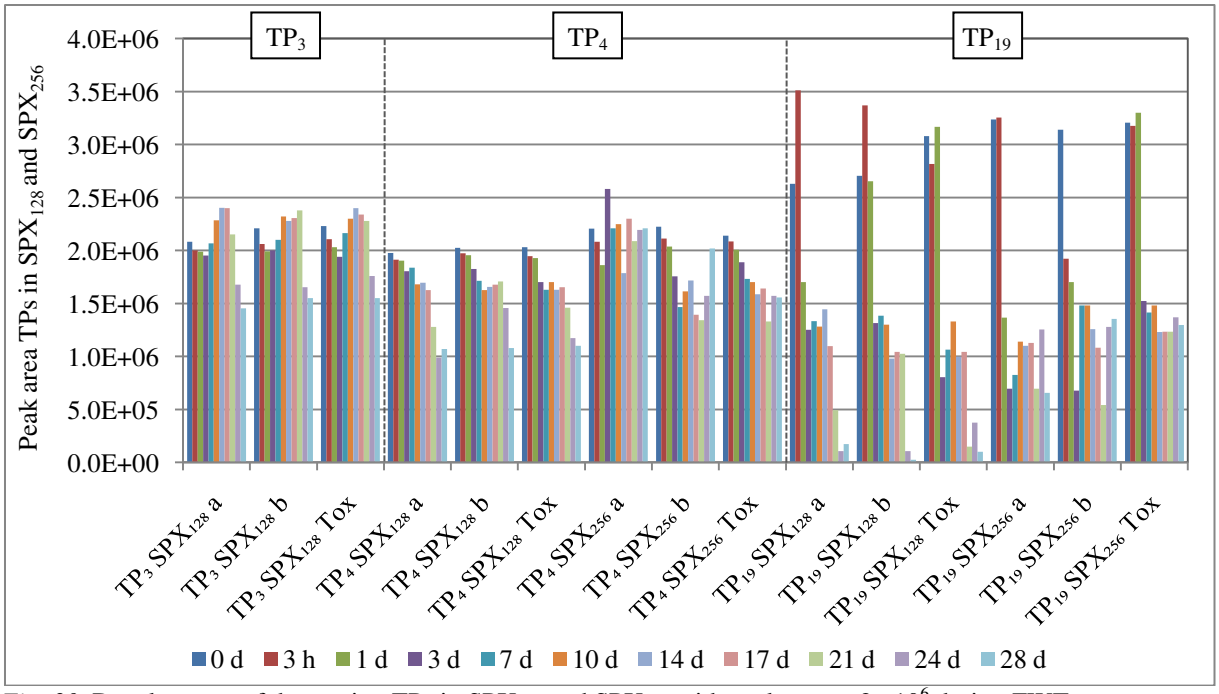

Fig. 30: Development of decreasing TPs in SPX_{128} and SPX_{256} with peak area > $2 \cdot 10^6$ during ZWT over test duration of 28 days

Reasons why several TPs were only degraded in some bottles can include different initial concentrations of the TPs, as well as the aforementioned processes of cometabolism and competitive inhibition. Furthermore, mutations occurring in the microbial communities must be considered. Bacterial strains being able to use the substrate as a source of carbon for biomass growth experience exponential population growth. Thus, mutations supporting the ability for degradation are facilitated. These mutations might not occur in all bottles to the same degree, leading to different levels of degradation.

4.4. Implications for "Benign by Design"

To target the described problem of the persistence of antibiotics in the environment, a wide range of proposed measures exists. These include short-term and medium-term measures like the improvement of technical processes to remove trace substances in WWTPs or the change of prescriptions to more environmentally friendly drugs (Klatte et al., 2017). In the long run, however, the new development or redesign of pharmaceuticals should be targeted, which is conducted by the "Benign by Design" concept (Leder et al., 2015). In these experiments, the non-targeted derivatisation through UV irradiation led to a wide variety of up to 41 detected photo-TPs. Concerning the pharmacological properties, no statements about potential changes can be derived from the experiments conducted with SPX. The established findings contribute to facilitating knowledge about changes in biodegradability which are induced by the photolysis of the parent compound. Even though SPX showed biodegradability during the ZWT in SPX_0 and SPX_{128}, this degradation only took place after at least 21 test days and

could not be observed in all test bottles. Consequently, TPs displaying a faster degradation taking place in all ZWT test bottles are potential candidates to be considered as more environmentally friendly derivatives of SPX. While none of the detected TPs could be degraded completely, several TPs showed continuous biodegradation throughout the test duration in all ZWT bottles. TP_4, TP_{10} and TP_{19} were the only TPs displaying substantial degradation in all six test bottles with photolysis solution and are therefore the most promising substances. A special emphasis can be put on TP_{19} which was nearly completely degraded in SPX_{128}. It should be noted that while no exact statements about the present concentrations of SPX and its TPs can be made, the peak areas of all relevant TPs were substantially smaller than the peak areas of SPX in the bottles where SPX was degraded. It can therefore be assumed that the degraded TPs have gained the characteristic of being biodegradable at lower concentrations. This is desirable when developing antibiotics which should be removable in the environment (Kümmerer, 2007). Especially TP_4, TP_{10} and TP_{19} should therefore be selected for further experiments. TP_3, TP_8, TP_{24} and TP_{25} were not degraded in all ZWT bottles and are hence not the most promising structures, but should still be included in further experiments.

However, it should be considered that the concentrations of test substances as well as the density of bacterial communities in the aquatic environment are considerably lower than those applied in the ZWT. Therefore, it cannot be assumed that SPX and the emerging derivatives will display the same degradation behaviour as observed in the ZWT.

5. Conclusion

In this thesis, the biodegradability of SPX and its photo-TPs, which were formed through UV irradiation, was determined by applying the CBT and the ZWT. As expected, SPX displayed a high photoreactivity when exposed to UV light and was degraded in a first-order reaction while a variety of photo-TPs was formed. The irradiation with UV light thus proved to be an efficient method for non-targeted derivatisation. During the CBT, neither SPX nor any of the photo-TPs were readily biodegradable. The tendency of FQs for substantial and pH dependent adsorption led to difficulties when determining the biodegradation in the ZWT through DOC measurements. A more frequent (e.g. daily) adjustment of the pH value during the test duration could potentially minimise this effect. However, HPLC analysis allowed insights into the degradation of SPX and its photo-TPs. SPX was degraded in SPX_0 and SPX_{128} during the last week of the ZWT, while no substantial degradation was observed in SPX_{256}. Several new bio-TPs emerged in all bottles and several TPs increased during the test. The most crucial TPs

were those displaying potentially improved degradability in the ZWT through abiotic and biotic processes. Especially TP_4, TP_{10} and TP_{19} which displayed biodegradation in all test bottles are of interest for the "Benign by Design" approach. Their potentially improved biodegradability is one of the characteristics which is targeted for the development of environmentally friendly pharmaceuticals. These results are of relevance even though the use of SPX has been widely decreased due to its phototoxic effects (Ball, 2000). The TPs might not retain these unwanted side effects and could lead to increased applicability of the drug. With no previous studies having been performed on the biodegradability of photo-TPs resulting from SPX, this thesis contributes to the assessment of the substance and environmental behaviour of antibiotics in general. Furthermore, even though the degradation of substances only occurred at higher substance concentrations and bacterial densities than present in the environment, the results can contribute to the knowledge on structure-related biodegradability of compounds. Therefore, the structure of the TPs displaying degradation through abiotic or biotic processes should be determined through mass spectrometry.

This experimental data on the biodegradability of compounds is necessary for the improvement of computational modelling and the prediction of biodegradability. These methods are gaining importance for the development of chemicals in accordance with the "Benign by Design" approach. Due to the extremely high number of different produced chemicals, it is not possible to conduct the time-consuming biodegradation experiments for every substance, but they are the basis for the prediction of biodegradability through *in silico* methods (Rücker & Kümmerer, 2012). To further characterise the compounds displaying potentially improved biodegradability, future research could determine their pharmacological properties. By applying *in silico* methods of QSAR and molecular docking, it can be elucidated whether the TPs display similar pharmacological activity to the parent compound (Leder et al., 2015). Furthermore, the acute and chronic ecotoxicity as well as human toxicity of the specific TPs is of interest to assess their impact and their potential for the "Benign by Design" approach (Rastogi et al., 2014).

6. Literature

Aldred, K. J., Kerns, R. J., & Osheroff, N. (2014). Mechanism of quinolone action and resistance. *Biochemistry*, *53*(10), 1565–1574.

Alexander, M. (1999). *Biodegradation and bioremediation* (2nd ed.). San Diego, CA, London, UK: Academic Press.

Amitai, S., Yassin, Y., & Engelberg-Kulka, H. (2004). MazF-mediated cell death in Escherichia coli: A point of no return. *Journal of Bacteriology*, *186*(24), 8295–8300.

Amorim, C. L., Maia, A. S., Mesquita, R. B. R., Rangel, A. O., van Loosdrecht, M. C. M., Tiritan, M. E., & Castro, P. M. L. (2014). Performance of aerobic granular sludge in a sequencing batch bioreactor exposed to ofloxacin, norfloxacin and ciprofloxacin. *Water Research*, *50*, 101–113.

Arnold, W. A., & McNeill, K. (2007). Chapter 3.2 Transformation of pharmaceuticals in the environment: Photolysis and other abiotic processes. In M. Petrovic & D. Barceló (Eds.), *Analysis, fate and removal of pharmaceuticals in the water cycle* (pp. 361–385). (Comprehensive Analytical Chemistry; Vol. 50).

Arsand, J. B., Hoff, R. B., Jank, L., Meirelles, L. N., Díaz-Cruz, M. S., Pizzolato, T. M., & Barceló, D. (2018). Transformation products of amoxicillin and ampicillin after photolysis in aqueous matrices: Identification and kinetics. *Science of the Total Environment*, *642*, 954–967.

aus der Beek, T., Weber, F.-A., Bergmann, A., Hickmann, S., Ebert, I., Hein, A., & Küster, A. (2016). Pharmaceuticals in the environment – Global occurrences and perspectives. *Environmental Toxicology and Chemistry*, *35*(4), 823–835.

Ball, P. (2000). Quinolone generations: Natural history or natural selection? *Journal of Antimicrobial Chemotherapy*, *46*(3), 17–24.

Bergheim, M., Gminski, R., Spangenberg, B., Debiak, M., Bürkle, A., Mersch-Sundermann, V., Kümmerer, K., Gieré, R. (2015). Antibiotics and sweeteners in the aquatic environment: Biodegradability, formation of phototransformation products, and in vitro toxicity. *Environmental Science and Pollution Research*, *22*(22), 18017–18030.

Bergmann, A., Fohrmann, R., & Weber, F.-A. (2011). *Zusammenstellung von Monitoringdaten zu Umweltkonzentrationen von Arzneimitteln*. Dessau-Roßlau, DE: Umweltbundesamt.

Bhatt, P., Mathur, N., Singh, A., & Bhatnagar, P. (2015). Recycled sewage sludge: A step to sustainable agriculture. *International Journal of Chemical Science*, *13*, 1611–1620.

Biswas, N. R., Verma, K., Gupta, S. K., Velpandian, T. (2009). Fluoroquinolones and other antibiotics. In A. K. Gupta & V. Krishna (Eds.), *Clinical ophthalmology: Contemporary perspectives* (9th ed., pp. 105-122). Uttar Pradesh, IN: Elsevier.

Bunge, M., & Lechner, U. (2009). Anaerobic reductive dehalogenation of polychlorinated dioxins. *Applied Microbiology and Biotechnology*, *84*(3), 429–444.

Čvančarová, M., Moeder, M., Filipová, A., & Cajthaml, T. (2015). Biotransformation of fluoroquinolone antibiotics by ligninolytic fungi – Metabolites, enzymes and residual antibacterial activity. *Chemosphere*, *136*, 311–320.

Domagala, J. M. (1994). Structure-activity and structure-side-effect relationships for the quinolone antibacterials. *Journal of Antimicrobial Chemotherapy*, *33*(4), 685–706.

Elbert, J. E., & Logue, B. A. (1999). Investigation of the photochemistry and photophysics of para-substituted tertiary thiocinnamamides. *Journal of Photochemistry and Photobiology A: Chemistry*, *128*(1-3), 85–92.

Engler, M., Rüsing, G., Sörgel, F., & Holzgrabe, U. (1998). Defluorinated sparfloxacin as a new photoproduct identified by liquid chromatography coupled with UV detection and tandem mass spectrometry. *Antimicrobial Agents and Chemotherapy*, *42*(5), 1151–1159.

Fatta-Kassinos, D., Vasquez, M. I., & Kümmerer, K. (2011). Transformation products of pharmaceuticals in surface waters and wastewater formed during photolysis and advanced oxidation processes–degradation, elucidation of byproducts and assessment of their biological potency. *Chemosphere*, *85*(5), 693–709.

FDA (2016). *FDA drug safety communication: FDA updates warnings for oral and injectable fluoroquinolone antibiotics due to disabling side effects.* U.S. Food and Drug Administration. Retrieved from https://www.fda.gov/media/119537/download, last accessed 31.07.2019.

Ferrando-Climent, L., Rodriguez-Mozaz, S., & Barceló, D. (2014). Incidence of anticancer drugs in an aquatic urban system: From hospital effluents through urban wastewater to natural environment. *Environmental Pollution*, *193*, 216–223.

Friedrich, J. (2010). *Untersuchung der Abbaubarkeit von Pharmazeutika und Chemikalien in einem optimierten Abbautest – Vergleich der Elektrodenmethode nach Clark mit einem auf dynamischer Lumineszenzlöschung basierenden Optrodenverfahren zur Messung der Sauerstoffkonzentration im Closed Bottle Test*. Freiburg im Breisgau, DE: Albert-Ludwigs-Universität.

Gaskins, H. R., Collier, C. T., & Anderson, D. B. (2002). Antibiotics as growth promotants: Mode of action. *Animal Biotechnology*, *13*(1), 29–42.

Hamscher, G., & Hartung, J. (2008). Veterinary antibiotics in dust: Sources, environmental con-centrations, and possible health hazards. In K. Kümmerer (Ed.), *Pharmaceuticals in the environment. Sources, fate, effects, and risks* (3rd ed., pp. 95–102). Berlin, DE: Springer.

Heit, G., Neuner, A., Saugy, P.-Y., & Braun, A. M. (1998). Vacuum-UV (172 nm) actinometry. The quantum yield of the photolysis of water. *The Journal of Physical Chemistry*, *102*(28), 5551–5561.

Hubicka, U., Żuromska-Witek, B., Żmudzki, P., Maślanka, A., Kwapińska, N., & Krzek, J. (2013). Determination of sparfloxacin and its photodegradation products by thin-layer chromatography with densitometry detection. Kinetic evaluation of the degradation process and identification of photoproduct by mass spectrometry. *Analytical Methods*, *5*(23), 6734–6740.

Jia, Y., Zhang, H., Khanal, S. K., Yin, L., & Lu, H. (2019). Insights into pharmaceuticals removal in an anaerobic sulfate-reducing bacteria sludge system. *Water Research*, *161*, 191–201.

Kawabata, K., Sugihara, K., Sanoh, S., Kitamura, S., & Ohta, S. (2013). Photodegradation of pharmaceuticals in the aquatic environment by sunlight and UV-A,-B and-C irradiation. *The Journal of Toxicological Sciences*, *38*(2), 215–223.

Kimmitt, P. T., Harwood, C. R., & Barer, M. R. (2000). Toxin gene expression by shiga toxin-producing Escherichia coli: The role of antibiotics and the bacterial SOS response. *Emerging Infectious Diseases*, *6*(5), 458.

Klatte, S., Schaefer, H.-C., & Hempel, M. (2017). Pharmaceuticals in the environment – A short review on options to minimize the exposure of humans, animals and ecosystems. *Sustainable Chemistry and Pharmacy*, *5*, 61–66.

Kümmerer, K., & Al-Ahmad, A. (1997). Biodegradability of the anti-tumour agents 5-fluorouracil, cytarabine, and gemcitabine: Impact of the chemical structure and synergistic toxicity with hospital effluent. *Acta Hydrochimica et Hydrobiologica*, *25*(4), 166–172.

Kümmerer, K., Al-Ahmad, A., & Mersch-Sundermann, V. (2000a). Biodegradability of some antibiotics, elimination of the genotoxicity and affection of wastewater bacteria in a simple test. *Chemosphere*, *40*(7), 701–710.

Kümmerer, K., Al-Ahmad, A., Bertram, B., & Wießler, M. (2000b). Biodegradability of antineoplastic compounds in screening tests: Influence of glucosidation and of stereochemistry. *Chemosphere*, *40*(7), 767–773.

Kümmerer, K. (2007). Sustainable from the very beginning: Rational design of molecules by life cycle engineering as an important approach for green pharmacy and green chemistry. *Green Chemistry*, *9*(8), 899–907.

Kümmerer, K. (2008). Pharmaceuticals in the environment – A brief summary. In K. Kümmerer (Ed.), *Pharmaceuticals in the environment. Sources, fate, effects, and risks* (3rd ed., pp. 3–21). Berlin, DE: Springer.

Kümmerer, K. (2009). Antibiotics in the aquatic environment – A review – Part I. *Chemosphere*, *75*(4), 417–434.

Landry, G. M., Dunning, C. L., Conrad, T., Hitt, M. J., & McMartin, K. E. (2013). Diglycolic acid inhibits succinate dehydrogenase activity in human proximal tubule cells leading to mitochondrial dysfunction and cell death. *Toxicology Letters*, *221*(3), 176–184.

Ledakowicz, S., Drozdek, E., Boruta, T., Foszpańczyk, M., Olak-Kucharczyk, M., Żyłła, R., & Gmurek, M. (2019). Impact of hydrogen peroxide on the UVC photolysis of diclofenac and toxicity of the phototransformation products. *International Journal of Photoenergy*, *2019*.

Leder, C., Rastogi, T., & Kümmerer, K. (2015). Putting benign by design into practice – Novel concepts for green and sustainable pharmacy: Designing green drug derivatives by non-targeted synthesis and screening for biodegradability. *Sustainable Chemistry and Pharmacy*, *2*, 31–36.

Leder, C., Suk, M., Lorenz, S., & Kümmerer, K. (2018). *Entwicklung eines umweltverträglichen Antibiotikums: Abschlussbericht 2018.* Lüneburg, DE: Institut für Nachhaltige Chemie und Umweltchemie, Leuphana Universität. Retrieved from https://www.dbu.de/OPAC/ab/DBU-Abschlussbericht-AZ-30839.pdf, last accessed 31.07.2019.

Li, B., & Zhang, T. (2010). Biodegradation and adsorption of antibiotics in the activated sludge process. *Environmental Science & Technology*, *44*(9), 3468–3473.

Li, W., Guo, C., Su, B., & Xu, J. (2012). Photodegradation of four fluoroquinolone compounds by titanium dioxide under simulated solar light irradiation. *Journal of Chemical Technology & Biotechnology*, *87*(5), 643–650.

Łukaszewicz, P., Kumirska, J., Bialk-Bielinska, A., Maszkowska, J., Mioduszewska, K., Puckowski, A., & Stepnowski, P. (2016). Application of high performance liquid chromatography for hydrolytic stability assessment of selected antibiotics in aqueous environment. *Current Analytical Chemistry*, *12*(4), 324–329.

Maia, A. S., Ribeiro, A. R., Amorim, C. L., Barreiro, J. C., Cass, Q. B., Castro, P. M. L., & Tiritan, M. E. (2014). Degradation of fluoroquinolone antibiotics and identification of metabolites/transformation products by liquid chromatography – tandem mass spectrometry. *Journal of Chromatography*, *1333*, 87–98.

Maia, A. S., Castro, P. M. L., & Tiritan, M. E. (2016). Integrated liquid chromatography method in enantioselective studies: Biodegradation of ofloxacin by an activated sludge consortium. *Journal of Chromatography*, *1029*, 174–183.

Martin-Laurent, F., Topp, E., Billet, L., Batisson, I., Malandain, C., Besse-Hoggan, P., Morin, S., Artigas, J., Bonnineau, C., Kergoat, L. (2019). Environmental risk assessment of antibiotics in agroecosystems: Ecotoxicological effects on aquatic microbial communities and dissemination of antimicrobial resistances and antibiotic biodegradation potential along the soil-water continuum. *Environmental Science and Pollution Research*, *26*(18), 18930–18937.

OECD (1992a). *Test No. 301, Ready biodegradability: OECD guideline for testing of chemicals.* Paris, FR: OECD Publishing. Retrieved from https://www.oecd-ilibrary.org/test-no-301-ready-biodegradability_5lmqcr2k7qmw.pdf?itemId=%2Fcontent%2Fpublication%2F9789264070349-en&mimeType=pdf, last accessed 31.07.2019.

OECD (1992b). *Test No. 302 b, Inherent biodegradability: Zahn-Wellens/EMPA-Test: OECD guideline for testing of chemicals.* Paris, FR: OECD Publishing. Retrieved from https://www.oecd-ilibrary.org/test-no-302b-inherent-biodegradability-zahn-wellens-evpa-test_5lmqcr2k7qg6.pdf?itemId=%2Fcontent%2Fpublication%2F9789264070387-en&mimeType=pdf, last accessed 31.07.2019.

Pan, X.-H., Bai, S.-P., Li, K.-W., Tao, X.-H., Zhang, Y., Zhang, Y.-C., Zhang, R.-M., Liu, F. (2014). Synthesis of three fluoroquinolone compounds. *Asian Journal of Chemistry*, *26*(24), 8586–8588.

Pankuch, G. A., Lichtenberger, C., Jacobs, M. R., & Appelbaum, P. C. (1996). Antipneumococcal activities of RP 59500 (quinupristin-dalfopristin), penicillin G, erythromycin, and sparfloxacin determined by MIC and rapid time-kill methodologies. *Antimicrobial Agents and Chemotherapy*, *40*(7), 1653–1656.

Rastogi, T., Leder, C., & Kümmerer, K. (2014). Designing green derivatives of β-blocker metoprolol: A tiered approach for green and sustainable pharmacy and chemistry. *Chemosphere*, *111*, 493–499.

Rathbun, R. E. (2000). Transport, behavior, and fate of volatile organic compounds in streams. *Critical Reviews in Environmental Science and Technology*, *30*(2), 129–295.

Real, F. J., Acero, J. L., Benitez, F. J., Roldán, G., & Fernández, L. C. (2010). Oxidation of hydrochlorothiazide by UV radiation, hydroxyl radicals and ozone: Kinetics and elimination from water systems. *Chemical Engineering Journal*, *160*(1), 72–78.

Rubinstein, E. (2001). History of quinolones and their side effects. *Chemotherapy*, *47*(3), 3–8.

Rücker, C., & Kümmerer, K. (2012). Modeling and predicting aquatic aerobic biodegradation – A review from a user's perspective. *Green Chemistry*, *14*(4), 875–887.

Salgado, H. R. N., Moreno, P. R. H., Braga, A. L., & Schapoval, E. E. S. (2009). Photodegradation of sparfloxacin and isolation of its degradation products by preparative HPLC. *Revista de Ciencias Farmaceuticas Basica e Aplicada*, *26*(1), 47–54.

Taveira Parente, C. E., Souza Brito, E. M., Azeredo, A., Meire, R. O., & Malm, O. (2019). Fluoroquinolone antibiotics and their interactions in agricultural soils – A review. *Orbital: The Electronic Journal of Chemistry*, *11*(1), 42–52.

Tervahauta, T., Rani, S., Leal, L. H., Buisman, C. J. N., & Zeeman, G. (2014). Black water sludge reuse in agriculture: Are heavy metals a problem? *Journal of Hazardous Materials*, *274*, 229–236.

Thomaidi, V. S., Stasinakis, A. S., Borova, V. L., & Thomaidis, N. S. (2016). Assessing the risk associated with the presence of emerging organic contaminants in sludge-amended soil: A country-level analysis. *Science of the Total Environment*, *548*, 280–288.

Tominaga, F. K., dos Santos Batista, A. P., Teixeira, A. S. C., & Borrely, S. I. (2018). Degradation of diclofenac by electron beam irradiaton: Toxicitiy removal, by-products identification and effect of another pharmaceutical compound. *Journal of Environmental Chemical Engineering*, *6*(4), 4605–4611.

Trovó, A. G., Melo, S. A. S., & Nogueira, R. F. P. (2008). Photodegradation of the pharmaceuticals amoxicillin, bezafibrate and paracetamol by the photo-Fenton process – Application to sewage treatment plant effluent. *Journal of Photochemistry and Photobiology A: Chemistry*, *198*(2–3), 215–220.

Vasconcelos, T. G., Henriques, D. M., König, A., Martins, A. F., & Kümmerer, K. (2009). Photodegradation of the antimicrobial ciprofloxacin at high pH: Identification and biodegradability assessment of the primary by-products. *Chemosphere*, *76*(4), 487–493.

Vasquez, M. I., Hapeshi, E., Fatta-Kassinos, D., & Kümmerer, K. (2013). Biodegradation potential of ofloxacin and its resulting transformation products during photolytic and photocatalytic treatment. *Environmental Science and Pollution Research*, *20*(3), 1302–1309.

Wammer, K. H., Korte, A. R., Lundeen, R. A., Sundberg, J. E., McNeill, K., & Arnold, W. A. (2013). Direct photochemistry of three fluoroquinolone antibacterials: Norfloxacin, ofloxacin, and enrofloxacin. *Water Research*, *47*(1), 439–448.

Wang, L., Qiang, Z., Li, Y., & Ben, W. (2017). An insight into the removal of fluoroquinolones in activated sludge process: Sorption and biodegradation characteristics. *Journal of Environmental Sciences*, *56*, 263–271.

Yao, L., Wang, Y., Tong, L., Li, Y., Deng, Y., Guo, W., & Gan, Y. (2015). Seasonal variation of antibiotics concentration in the aquatic environment: A case study at Jianghan Plain, central China. *Science of the Total Environment*, *527*, 56–64.

Zhou, X., Zhang, Y., Shi, L., Chen, J., Qiang, Z., & Zhang, T. C. (2013). Partitioning of fluoroquinolones on wastewater sludge. *Clean – Soil, Air, Water*, *41*(8), 820–827.

7. Annex

List of Figures I
List of Tables II
A. Retention Times and Optimal Wavelengths for Measurement of TPs III
B. TPs ZWT in Sterile Controls IV
C. Peaks ZWT in BV and QC VI
D. TPs ZWT in SPX_{128} VI
E. TPs ZWT in SPX_{256} VIII

List of Figures

Fig. i: Development of TPs in SPX_0 St during ZWT over test duration of 28 days IV
Fig. ii: Development of TPs in SPX_{128} St with peak area < $2 \cdot 10^6$ during ZWT over test duration of 28 days V
Fig. iii: Development of TPs in SPX_{128} St with peak area > $2 \cdot 10^6$ during ZWT over test duration of 28 days V
Fig. iv: Development of TPs in SPX_{256} St with peak area < $2 \cdot 10^6$ during ZWT over test duration of 28 days V
Fig. v: Development of TPs in SPX_{256} St with peak area > $2 \cdot 10^6$ during ZWT over test duration of 28 days VI
Fig. vi: Development of peaks in BV and QC during ZWT over test duration of 28 days VI
Fig. vii: Development of TPs in SPX_{128} a with peak area < $1 \cdot 10^6$ during ZWT over test duration of 28 days VI
Fig. viii: Development of TPs in SPX_{128} a with peak area > $1 \cdot 10^6$ during ZWT over test duration of 28 days VII
Fig. ix: Development of TPs in SPX_{128} b with peak area < $1 \cdot 10^6$ during ZWT over test duration of 28 days VII
Fig. x: Development of TPs in SPX_{128} b with peak area > $1 \cdot 10^6$ during ZWT over test duration of 28 days VII
Fig. xi: Development of TPs in SPX_{128} Tox with peak area < $1 \cdot 10^6$ during ZWT over test duration of 28 days VIII
Fig. xii: Development of TPs in SPX_{128} Tox with peak area > $1 \cdot 10^6$ during ZWT over test duration of 28 days VIII
Fig. xiii: Development of TPs in SPX_{256} a with peak area < $5 \cdot 10^5$ during ZWT over test duration of 28 days VIII
Fig. xiv: Development of TPs in SPX_{256} a with peak area > $5 \cdot 10^5$ during ZWT over test duration of 28 days IX
Fig. xv: Development of TPs in SPX_{256} b with peak area < $5 \cdot 10^5$ during ZWT over test duration of 28 days IX
Fig. xvi: Development of TPs in SPX_{256} b with peak area > $5 \cdot 10^5$ during ZWT over test duration of 28 days IX

Fig. xvii: Development of TPs in SPX_{256} Tox with peak area < $5 \cdot 10^5$ during ZWT over test duration of 28 days X
Fig. xviii: Development of TPs in SPX_{256} Tox with peak area > $5 \cdot 10^5$ during ZWT over test duration of 28 days X

List of Tables

Tab. i: Retention times and optimal wavelengths for measurement of TPs detected during photodegradation III
Tab. ii: Retention times and optimal wavelengths for measurement of TPs detected during CBT and ZWT III

A. Retention Times and Optimal Wavelengths for Measurement of TPs

Tab. i: Retention times and optimal wavelengths for measurement of TPs detected during photodegradation

Substances 256 min irradiation	*Retention time[min]*	*Wave-length [nm]*	*Substances 496 min irradiation*	*Rentention time [min]*	*Wave-length [nm]*
SPX	15.345	298	SPX	15.366	298
TP_1	2.264	254	TP_1	2.275	255
TP_2	2.580	255	TP_2	2.598	255
TP_3	2.756	255	TP_5	10.678	287
TP_4	4.997	248	TP_6	11.239	282
TP_5	10.668	287	TP_7	12.076	294
TP_6	11.226	282	TP_8	12.139	288
TP_7	12.086	294	TP_9	12.391	289
TP_{10}	12.937	286	TP_{10}	12.911	286
TP_{11}	13.375	288	TP_{11}	13.383	288
TP_{12}	13.957	295	TP_{12}	13.948	295
TP_{13}	14.137	291	TP_{13}	14.139	291
TP_{14}	14.606	298	TP_{14}	14.603	298
TP_{17}	15.404	292	TP_{15}	14.839	292
TP_{18}	16.644	295	TP_{16}	15.159	289
TP_{19}	17.335	291	TP_{17}	15.392	289
TP_{20}	18.369	295	TP_{18}	16.591	295
			TP_{19}	17.331	295
			TP_{20}	18.348	295

Tab. ii: Retention times and optimal wavelengths for measurement of TPs detected during CBT and ZWT

Substances CBT	*Retention time [min]*	*Wave-length [nm]*	*Substances ZWT*	*Retention time [min]*	*Wave-length [nm]*
SPX	15.951	297	SPX	15.605	298
TP_1	2.690	254	TP_1	1.983	295
TP_2	3.019	254	TP_2	2.656	301
TP_3	3.317	254	TP_3	3.019	254
TP_4	3.508	254	TP_4	3.875	257
TP_5	3.860	254	TP_5	4.246	253
TP_6	5.052	254	TP_6	4.890	252
TP_7	5.589	254	TP_7	5.346	252
TP_8	6.689	254	TP_8	5.644	253
TP_9	8.791	250	TP_9	6.224	254
TP_{10}	11.060	263	TP_{10}	6.482	261
TP_{11}	11.364	245	TP_{11}	7.471	254
TP_{12}	12.254	292	TP_{12}	8.592	282
TP_{13}	13.041	285	TP_{13}	8.987	260
TP_{14}	13.536	288	TP_{14}	9.346	284
TP_{15}	14.080	297	TP_{15}	10.001	292
TP_{16}	14.259	289	TP_{16}	10.246	292
TP_{17}	14.694	292	TP_{17}	10.761	292
TP_{18}	14.922	292	TP_{18}	11.097	260
TP_{19}	15.573	290	TP_{19}	11.266	260

TP_{20}	17.366	292	TP_{20}	11.620	287
TP_{21}	18.388	292	TP_{21}	12.074	260
TP_{22}	18.956	283	TP_{22}	12.867	260
			TP_{23}	13.178	287
			TP_{24}	13.873	288
			TP_{25}	14.087	294
			TP_{26}	14.345	290
			TP_{27}	14.761	291
			TP_{28}	16.696	290
			TP_{29}	16.930	280
			TP_{30}	17.230	290
			TP_{31}	17.892	290
			TP_{32}	18.198	290
			TP_{33}	18.850	286
			TP_{34}	19.260	289
			TP_{35}	19.643	289
			TP_{36}	20.349	289
			TP_{37}	21.579	253
			TP_{38}	22.069	289
			TP_{39}	24.015	289
			TP_{40}	24.908	256
			TP_{41}	25.626	261

B. TPs ZWT in Sterile Controls

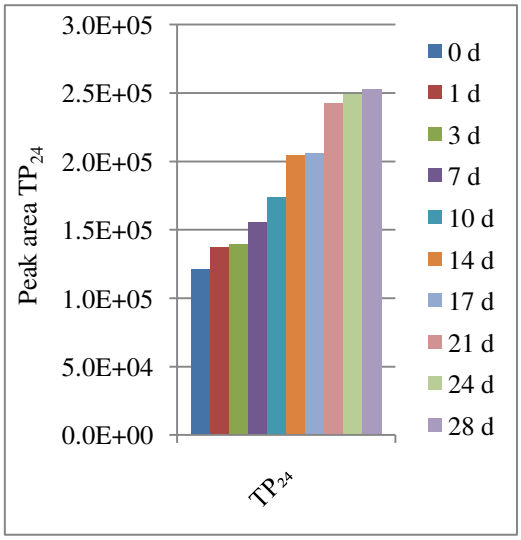

Fig. i: Development of TPs in SPX_0 St during ZWT over test duration of 28 days

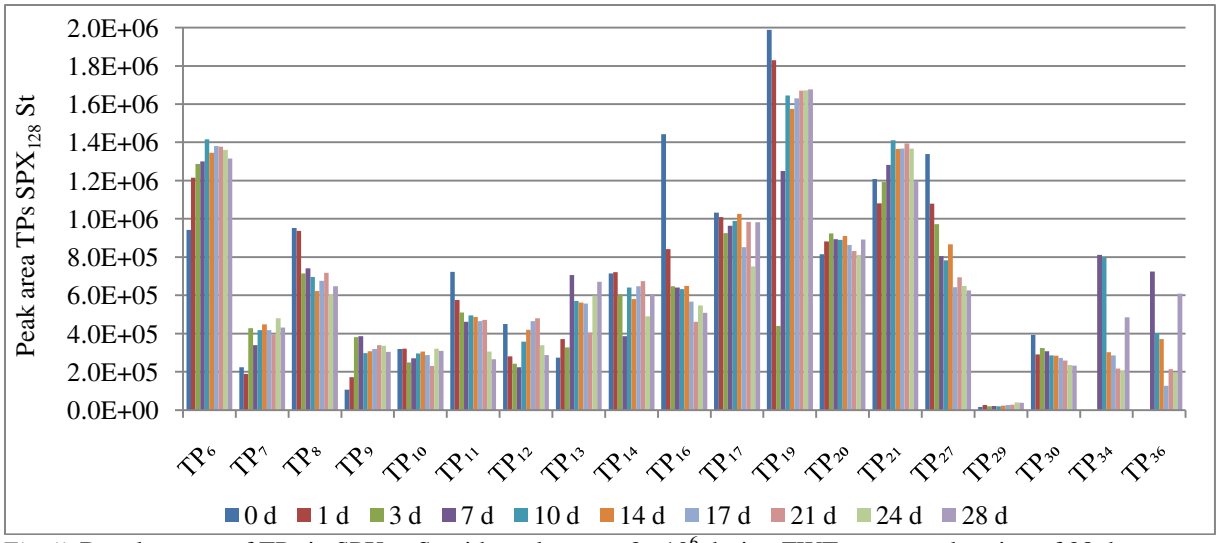

Fig. ii: Development of TPs in SPX_{128} St with peak area < $2 \cdot 10^6$ during ZWT over test duration of 28 days

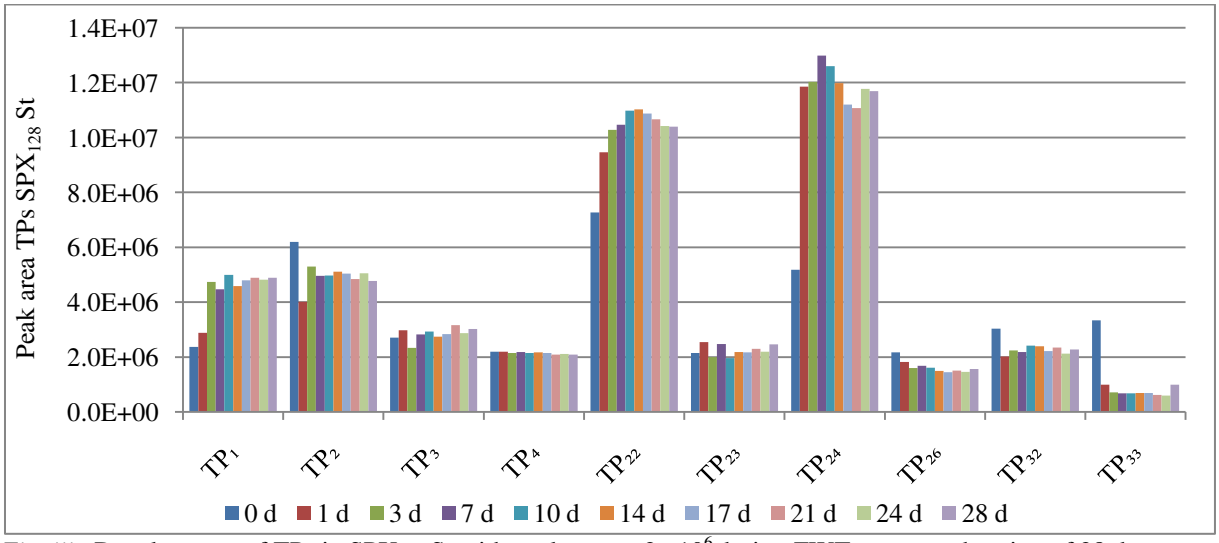

Fig. iii: Development of TPs in SPX_{128} St with peak area > $2 \cdot 10^6$ during ZWT over test duration of 28 days

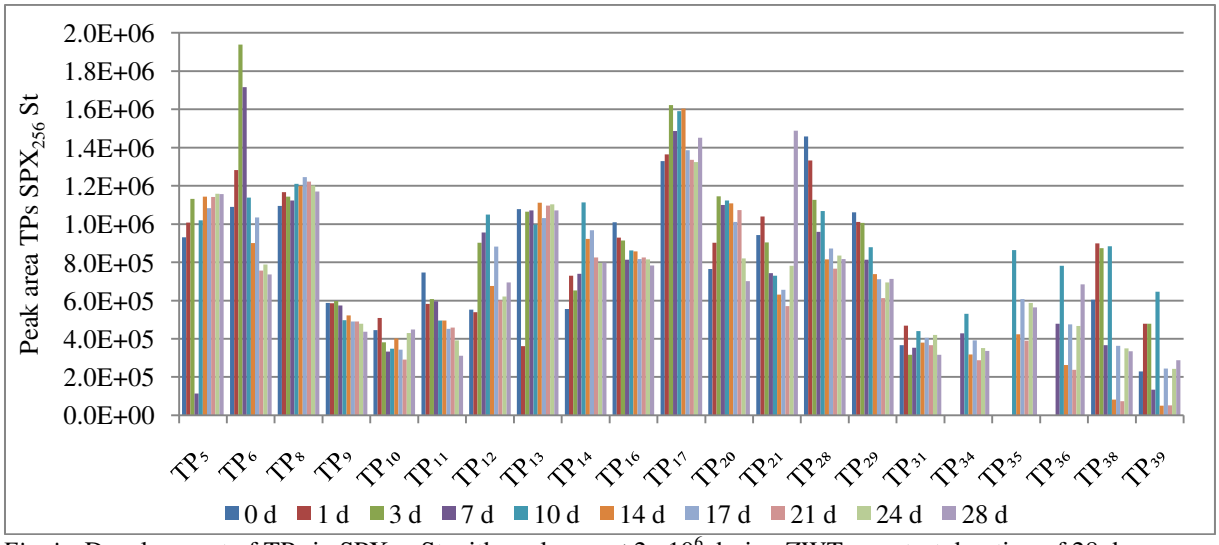

Fig. iv: Development of TPs in SPX_{256} St with peak area < $2 \cdot 10^6$ during ZWT over test duration of 28 days

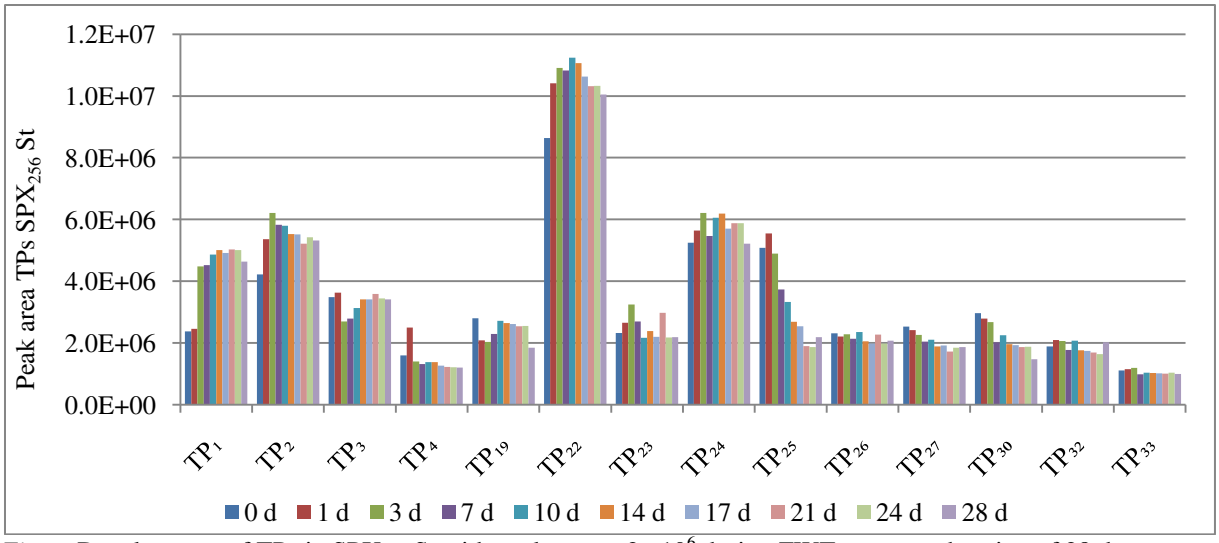

Fig. v: Development of TPs in SPX_{256} St with peak area > $2 \cdot 10^6$ during ZWT over test duration of 28 days

C. Peaks ZWT in BV and QC

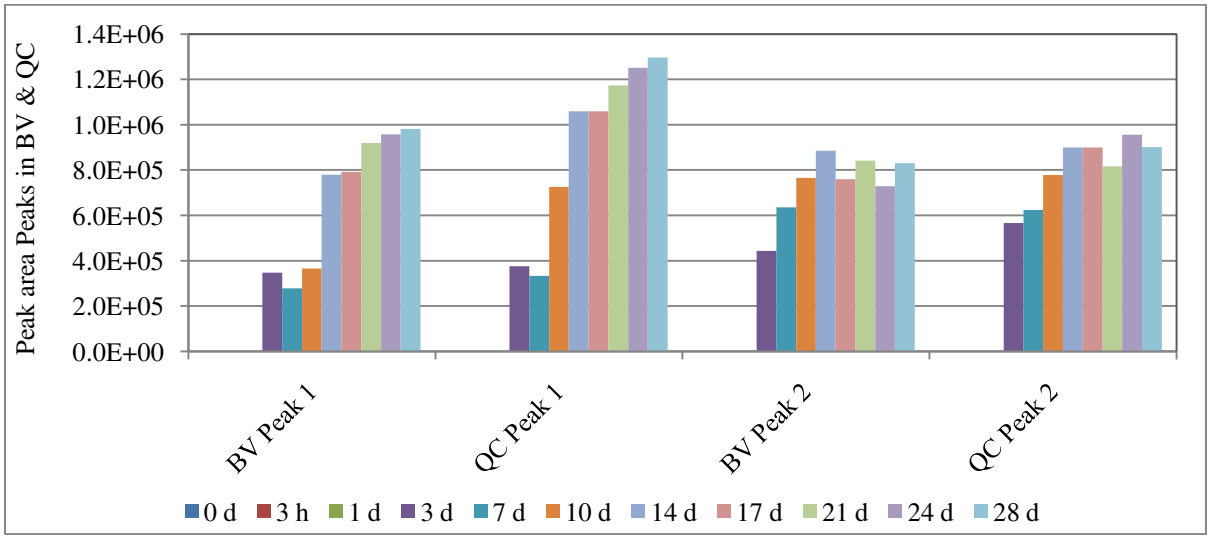

Fig. vi: Development of peaks in BV and QC during ZWT over test duration of 28 days

D. TPs ZWT in SPX_{128}

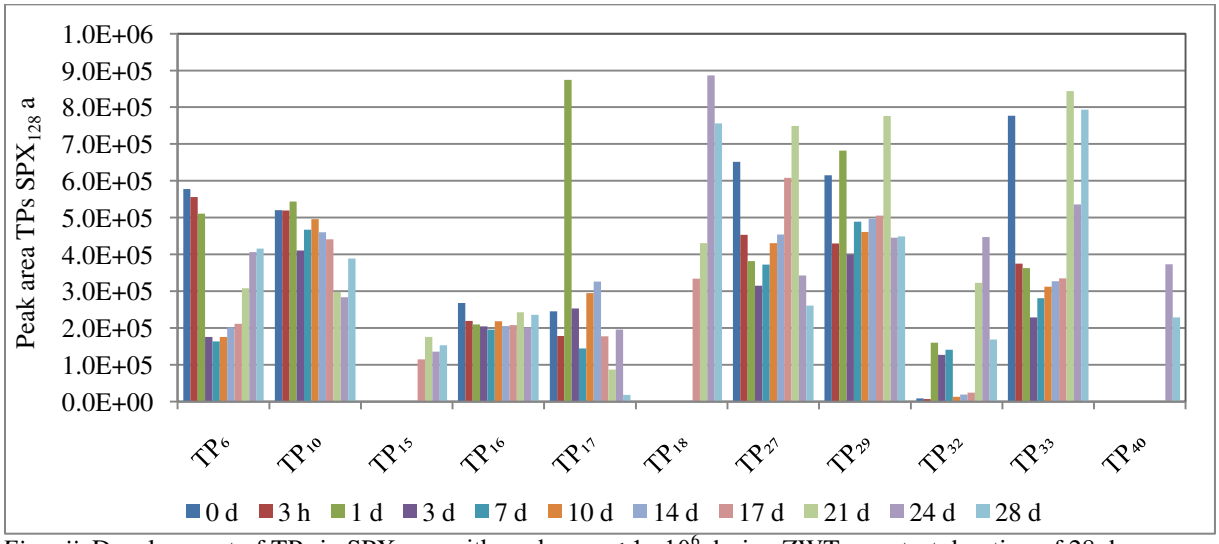

Fig. vii: Development of TPs in SPX_{128} a with peak area < $1 \cdot 10^6$ during ZWT over test duration of 28 days

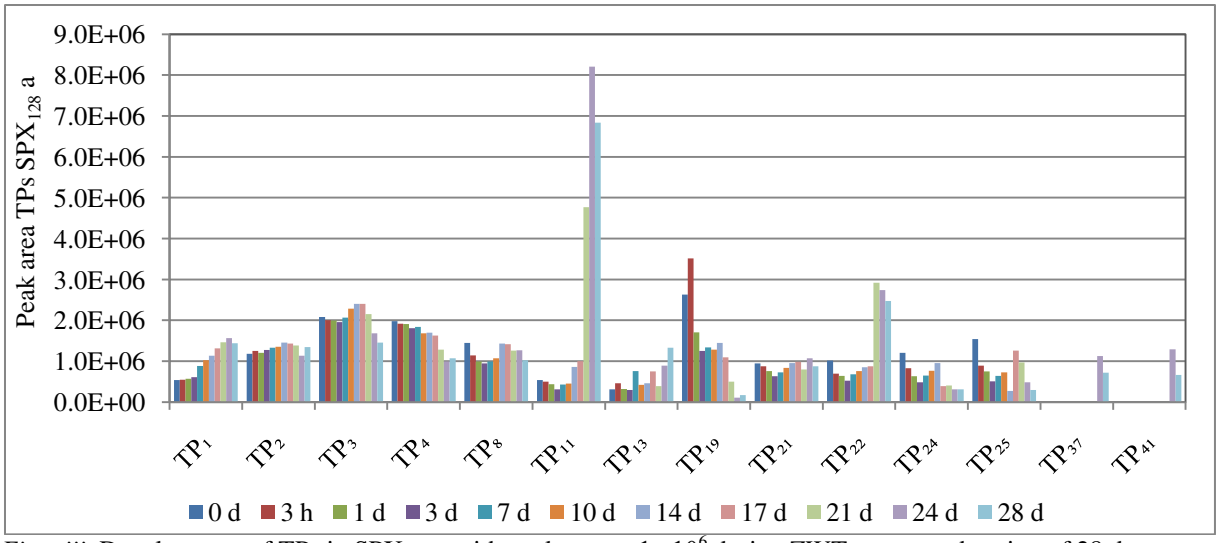

Fig. viii: Development of TPs in SPX_{128} a with peak area > $1 \cdot 10^6$ during ZWT over test duration of 28 days

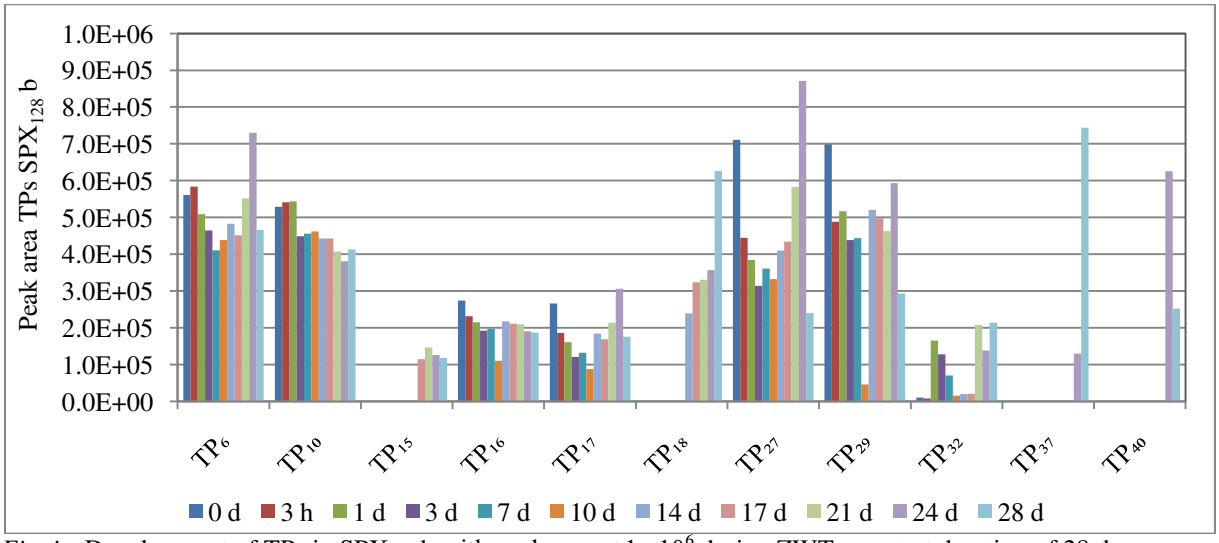

Fig. ix: Development of TPs in SPX_{128} b with peak area < $1 \cdot 10^6$ during ZWT over test duration of 28 days

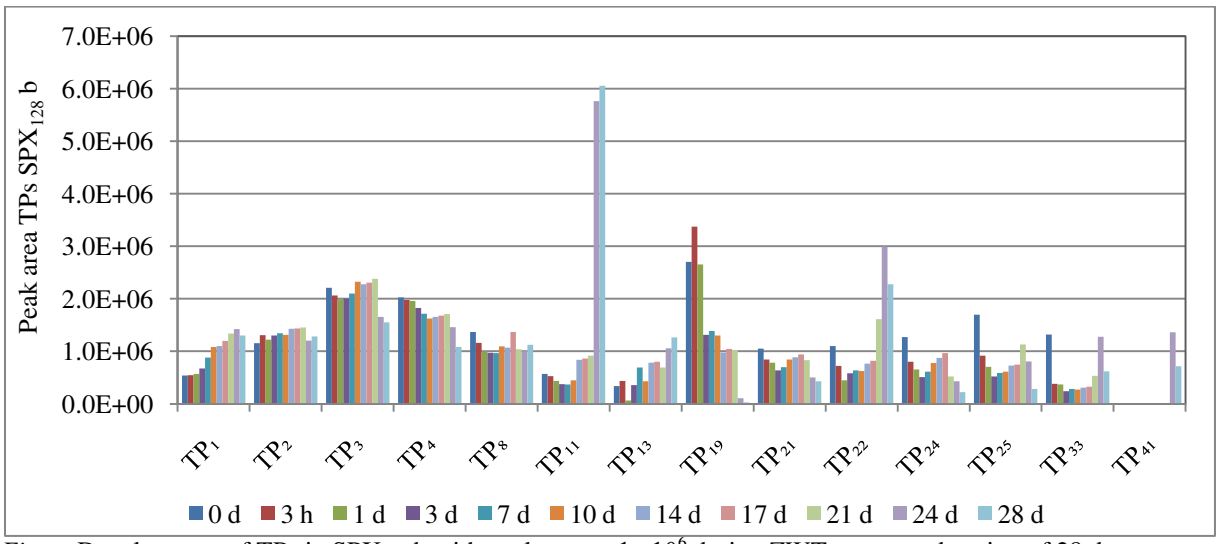

Fig. x: Development of TPs in SPX_{128} b with peak area > $1 \cdot 10^6$ during ZWT over test duration of 28 days

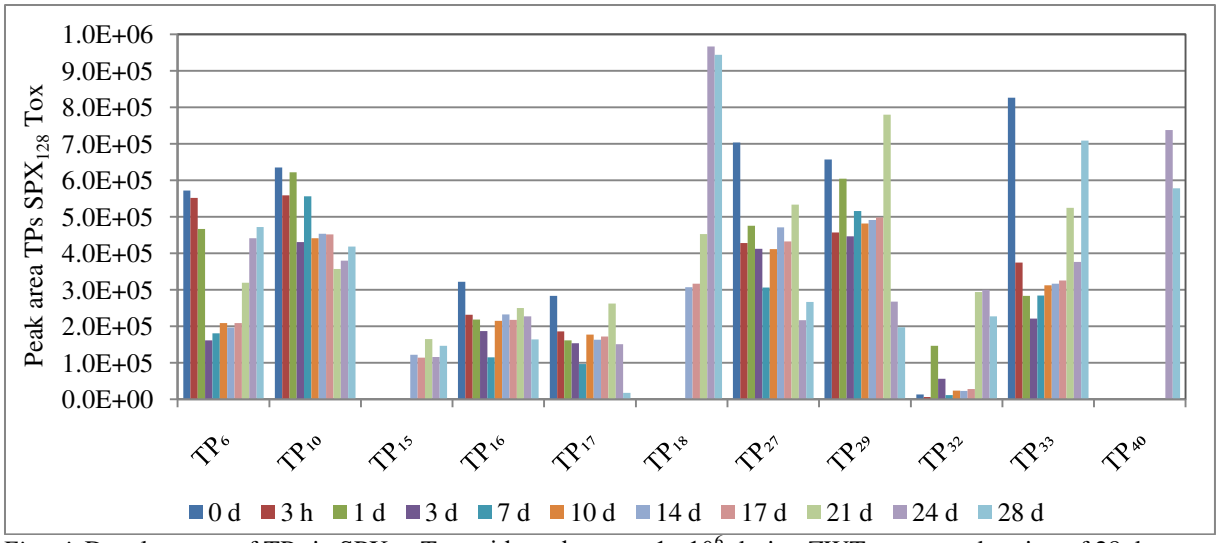

Fig. xi: Development of TPs in SPX_{128} Tox with peak area < $1 \cdot 10^6$ during ZWT over test duration of 28 days

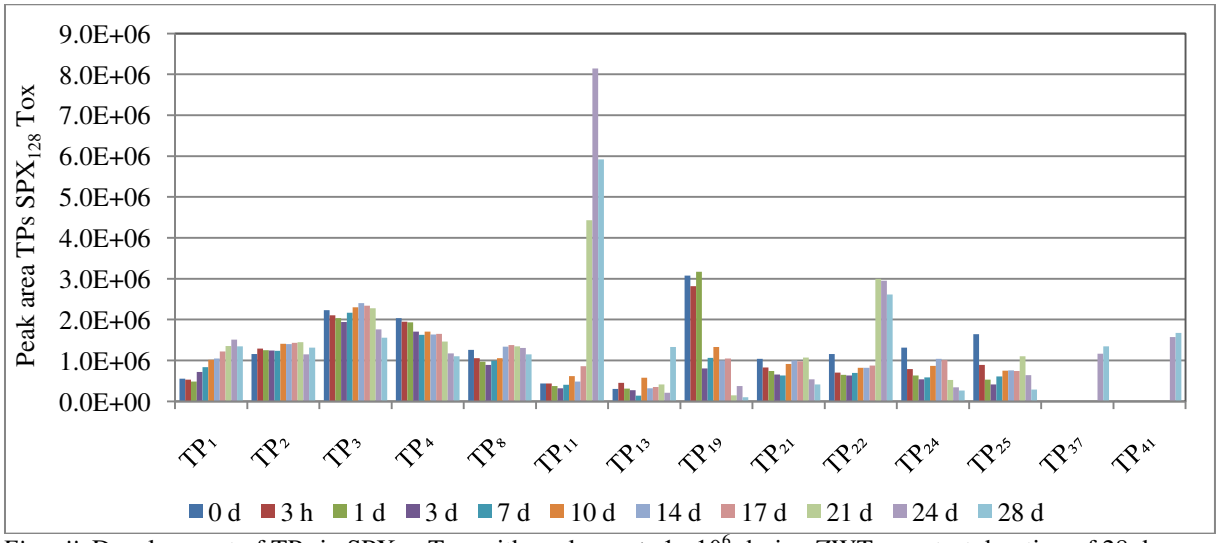

Fig. xii: Development of TPs in SPX_{128} Tox with peak area > $1 \cdot 10^6$ during ZWT over test duration of 28 days

E. TPs ZWT in SPX_{256}

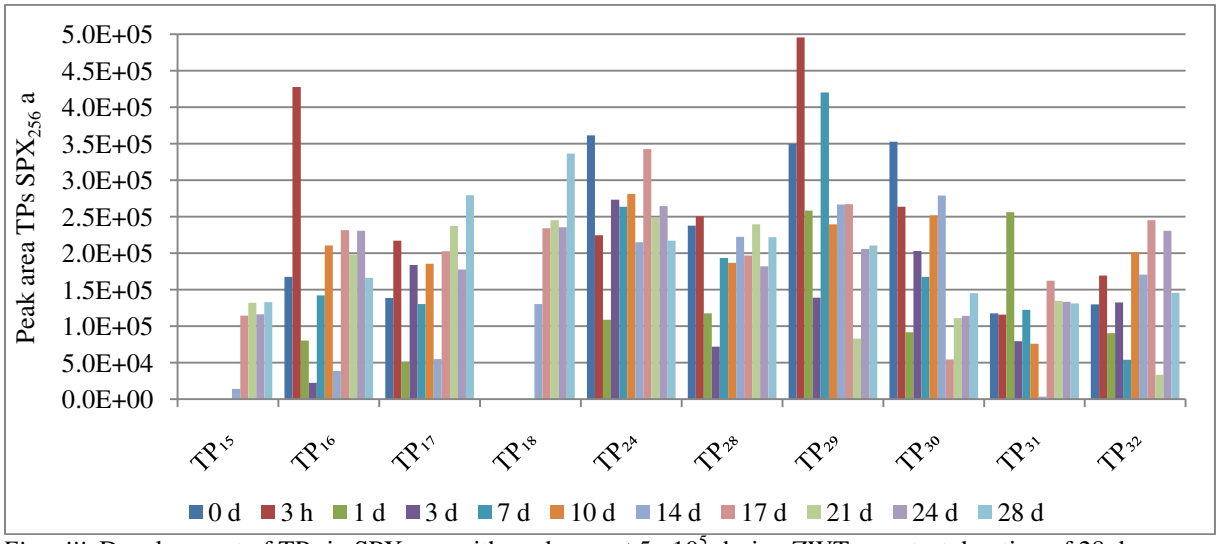

Fig. xiii: Development of TPs in SPX_{256} a with peak area < $5 \cdot 10^5$ during ZWT over test duration of 28 days

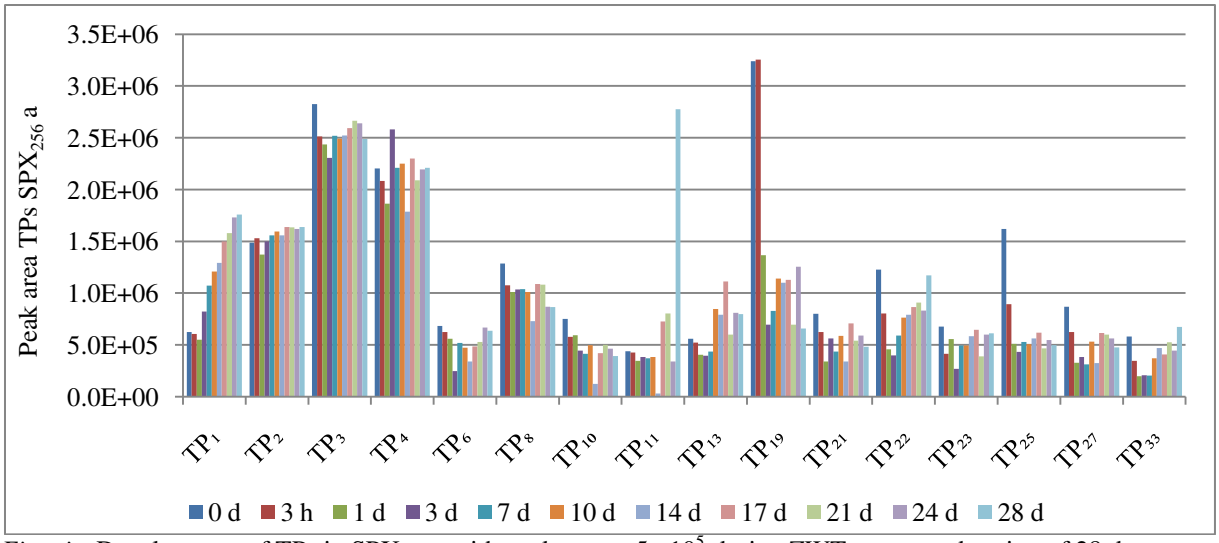

Fig. xiv: Development of TPs in SPX_{256} a with peak area > $5 \cdot 10^5$ during ZWT over test duration of 28 days

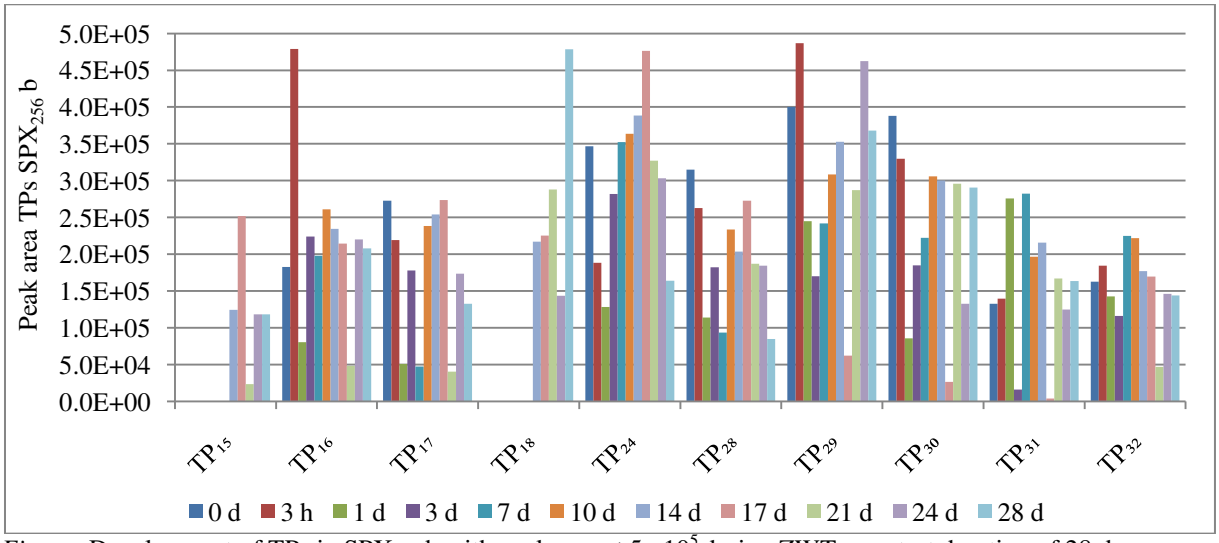

Fig. xv: Development of TPs in SPX_{256} b with peak area < $5 \cdot 10^5$ during ZWT over test duration of 28 days

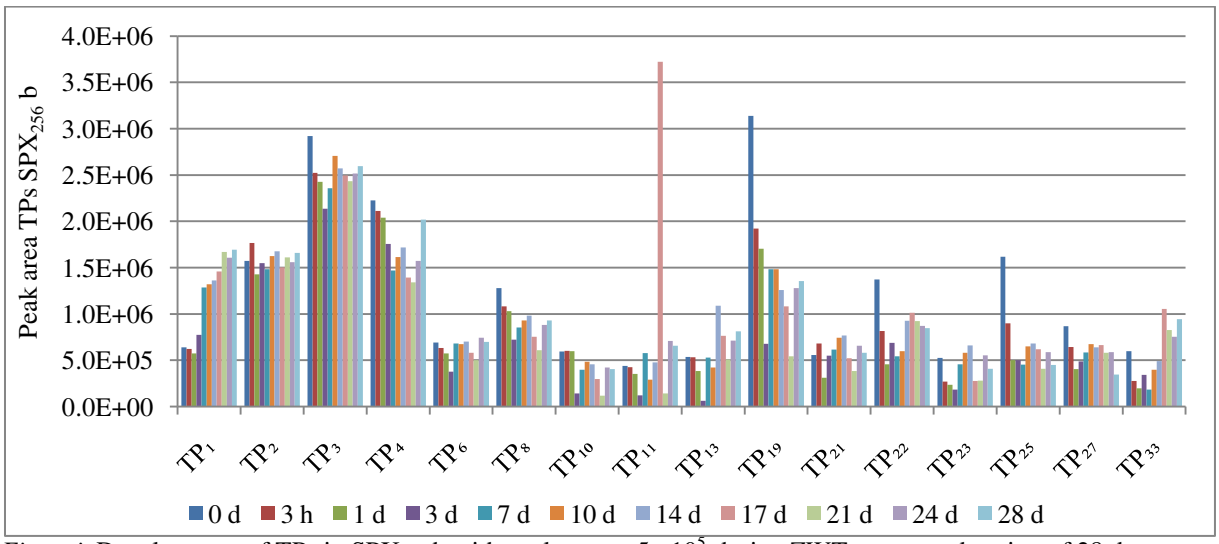

Fig. xvi: Development of TPs in SPX_{256} b with peak area > $5 \cdot 10^5$ during ZWT over test duration of 28 days

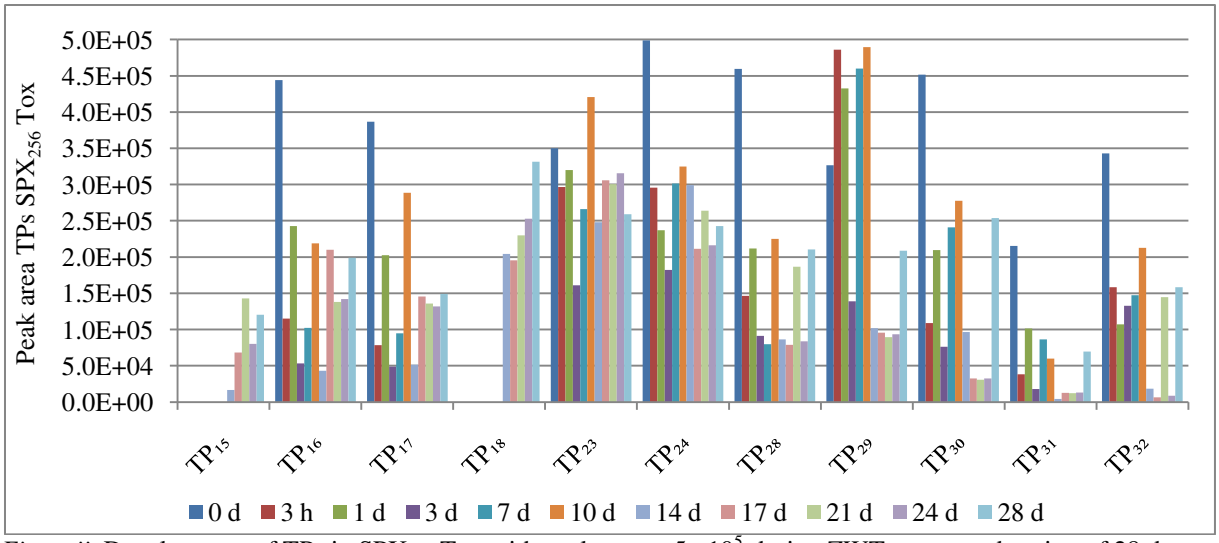

Fig. xvii: Development of TPs in SPX_{256} Tox with peak area < $5 \cdot 10^5$ during ZWT over test duration of 28 days

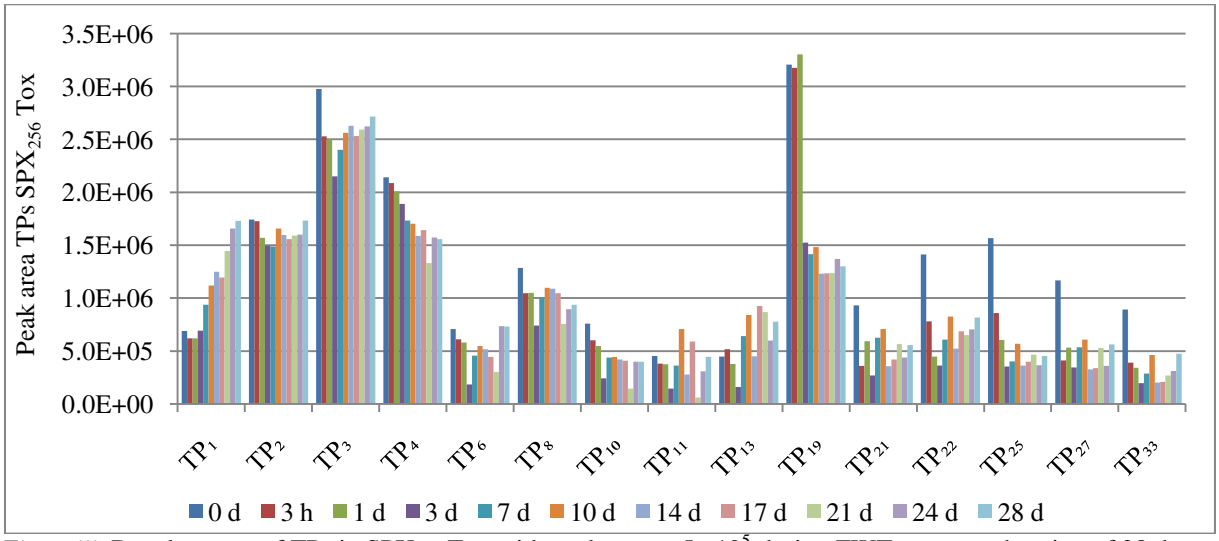

Fig. xviii: Development of TPs in SPX_{256} Tox with peak area > $5 \cdot 10^5$ during ZWT over test duration of 28 days

8. Declaration of Authorship

I hereby declare that

- I am the sole author of this bachelor thesis and I have not used any sources other than those listed in the bibliography and identified as references,
- all parts of this thesis which have been taken literally or analogously from other works have been identified as such,
- I have not submitted this thesis at any other institution.

_____

(Place, Date)

_____

(Signature)